Semiclassical theory of nonlocal statistical measures: Residual Coulomb interactions

Denis Ullmo,[1] Steven Tomsovic,[1,2,3] and Arnd Bäcker[4]
[1]*CNRS, Université Paris-Sud, LPTMS UMR 8626, 91405 Orsay Cedex, France*
[2]*Max-Planck-Institut für Physik komplexer Systeme, D-01187 Dresden, Germany*
[3]*Department of Physics and Astronomy, Washington State University, Pullman, Washington 99164-2814, USA* *
[4]*Institut für Theoretische Physik, Technische Universität Dresden, 01062 Dresden, Germany*
(Received 30 December 2008; published 15 May 2009)

In a recent paper [Phys. Rev. Lett. **100**, 164101 (2008)] and within the context of quantized chaotic billiards, random plane-wave and semiclassical theoretical approaches were applied to an example of a relatively new class of statistical measures, i.e., measures involving both complete spatial integration and energy summation as essential ingredients. A quintessential example comes from the desire to understand the short-range approximation to the first-order ground-state contribution of the residual Coulomb interaction. Billiards, fully chaotic or otherwise, provide an ideal class of systems on which to focus as they have proven to be successful in modeling the single-particle properties of a Landau-Fermi liquid in typical mesoscopic systems, i.e., closed or nearly closed quantum dots. It happens that both theoretical approaches give fully consistent results for measure averages, but that somewhat surprisingly for fully chaotic systems the semiclassical theory gives a much improved approximation for the fluctuations. Comparison of the theories highlights a couple of key shortcomings inherent in the random plane-wave approach. This paper contains a complete account of the theoretical approaches, elucidates the two shortcomings of the oft-relied-upon random plane-wave approach, and treats non-fully-chaotic systems as well.

DOI: 10.1103/PhysRevE.79.056217 PACS number(s): 05.45.Mt, 03.65.Sq, 71.10.Ay, 73.21.La

I. INTRODUCTION

Finite and low-dimensional quantum systems often possess statistical properties whose deviations from universality contain some basic dynamical information about the system [1–4]. A recurring challenge is to understand precisely what information is buried in those statistical deviations and how to extract it. Before that can be addressed, the universal behaviors themselves must be understood. At the heart of many such universalities generally lurks a connection to the Bohigas-Giannoni-Schmit (BGS) conjecture [5,6], which asserts that systems with underlying chaotic dynamics have the fluctuation properties found in random matrix theory [7]. If interest lies in quantities for which the position representation of the eigenfunctions is critical, a random plane-wave model is often introduced that augments the BGS conjecture [8,9]. The primary goal of extracting system specific information can then proceed, but generally requires a more powerful theory.

The preponderance of statistical measures heretofore introduced for analysis are local in energy, configuration space, or both. Examples are given by the Dyson-Mehta cluster functions [7], and the amplitude distribution and short-range two-point correlation function $c(|\mathbf{r}-\mathbf{r}'|)=\langle\psi(\mathbf{r})\psi(\mathbf{r}')\rangle$ of a given eigenfunction, $\psi(\mathbf{r})$. On the other hand, there has been a rather recent introduction of new nonlocal statistical measures [10–12]. They have been motivated by the need to understand the interplay between interferences and interactions in mesoscopic systems. For example, one place where this interplay is known to have an important role is the addition spectra of quantum dots; other examples are coming from cold fermionic gases. Focusing on just one motivation, the addition spectrum is experimentally accessible through the position of the conductance peaks in the Coulomb blockade transport measurements [13–18]. Fluctuations of peak spacings are associated with interference effects and experimentally are clearly incompatible with a noninteracting description of the conduction electrons in the dots. Indeed, except for very small dots with a circular symmetry [18] for which additional degeneracies are expected, a noninteracting description predicts a strong bimodality of the peak spacing distribution—associated with an odd-even character of the number of (spin-1/2) electrons—and this is not observed. Assuming further that the dot possesses a chaotic dynamics, the distribution for odd-N spacings should show a characteristic Wigner surmise shape, whereas a density similar to a Gaussian with extended tails is observed.

At first, it was argued that a non-Fermi-liquid description of the interacting electrons might be necessary to interpret the experimental data. However, the picture which has now emerged [19–23] is that although an understanding of both peak spacings and ground-state spin distributions is still incomplete, it is reasonable to expect that most phenomena will eventually be explained within a Fermi-liquid framework. More specifically, the electrons can be thought of as quasiparticles confined by a potential $U_{\mathrm{conf}}(\mathbf{r})$, which could in practice be computed within a self-consistent Thomas-Fermi-type approximation [24]. They also interact weakly through a screened Coulomb interaction $V_{\mathrm{sc}}(\mathbf{r},\mathbf{r}')$. For dots significantly larger than the screening length, confinement does not modify appreciably the screening process, and the bulk expression for $V_{\mathrm{sc}}(\mathbf{r}-\mathbf{r}')$ is appropriate. Furthermore, for the experimentally relevant gas parameter r_s being of order 1, the screening length is not much different from the Fermi wavelength λ_F. Under these circumstances, the problem is well described by the short-range approximation

*Permanent address.

$$V_{\rm sc}(\mathbf{r}-\mathbf{r}') = \frac{F_0^a}{\nu}\delta(\mathbf{r}-\mathbf{r}'), \tag{1}$$

with ν as the mean local density of states (including the spin degeneracy) ($\nu = m/\pi\hbar^2$ for $d=2$) and F_0^a as the dimensionless Fermi-liquid parameter [25] (for $d=2$ and r_s of order 1, F_0^a is in the range 0.6–0.8). Boundaries could potentially modify this picture somewhat, but it is expected that a slightly modified F_0^a would be sufficient to capture the effects; since this is not the focus of our study, we leave it for future consideration.

In this approximation, the first-order contribution of the residual interactions to the ground-state energy can be expressed in the simple form,

$$\delta E^{\rm RI} = \frac{F_0^a}{\nu}\int d\mathbf{r} n_\uparrow(\mathbf{r}) n_\downarrow(\mathbf{r}), \tag{2}$$

with n_σ as the unperturbed ground-state density of particles with spin σ. This expression was the starting point for a study demonstrating the increased importance of $\delta E^{\rm RI}$ if the dynamics are not fully chaotic [10].

Because $n_\sigma(\mathbf{r})$ can be expressed as a sum over the absolute square of single-particle eigenfunctions which are occupied, the mesoscopic fluctuations of the residual energy term $\delta E^{\rm RI}$ of Eq. (2), or of similar quantities, are related to the fluctuations of the one-particle eigenstates of the unperturbed system. However, in contrast to the correlation function $c(|\mathbf{r}-\mathbf{r}'|)$, Eq. (2) involves both an integration over space and summation over energy, and therefore in this way, it is probing new aspects of the fluctuation properties of the eigenstates.

The goal of this paper is to follow up on our recent work [26] on the average and fluctuating parts of the quantity in Eq. (2) in several ways. To begin with a complete account is given of two theoretical approaches using random plane waves and semiclassical theory. As already shown, for fully chaotic quantized billiards the two methods give identical leading functional dependence on wave vector and system size for average and fluctuation properties. In addition, the significant differences between Dirichlet and Neumann boundary conditions can be understood. On the other hand, in the statistical limit of uniformity, the fluctuation properties differ in two ways in the prefactor. The semiclassical treatment in the spirit of the Gutzwiller trace formula [27,28] helps identify dynamical correlations and a term missing from the expressions derived with the random plane-wave model. Thus, the Gutzwiller periodic orbit approach provides both a deeper understanding of the mechanism underlying the fluctuations and a good quantitative agreement with exact numerical calculations for the examples considered. Next, non-fully-chaotic systems are partially addressed. The fluctuations are found to be greatly magnified in two essential ways. One relates to nonuniform projected classical densities and the other to enhanced dependence on wave vector and system size.

The organization of the paper is as follows. In Sec. II, the necessary background material and notations are introduced, including a more precise definition of the statistical quantities to be studied. Also introduced in this section is the random plane-wave model, which is then used to analyze in Sec. III the mean and fluctuating behaviors. The random plane-wave modeling reproduces quite accurately the mean behaviors, but it fails by most of an order of magnitude to predict quantitatively the fluctuations. This motivates the introduction in Sec. IV of the semiclassical analysis in terms of classical trajectories. This approach corrects the random plane-wave method overestimate of the fluctuations. In Sec. V, extended semiclassical methods are introduced for systems which are not fully chaotic. Finally Sec. VI contains a discussion and summary.

II. PRELIMINARY CONSIDERATIONS

To begin, it is worth motivating the introduction of a nonlocal statistical measure in a little more detail. For example, consider two-degree-of-freedom chaotic quantized billiard systems with one-body eigenstates $\psi_i(\mathbf{r})$ and energies E_i. In the absence of interactions, the many-body eigenstates are Slater determinants characterized by spin-dependent occupation numbers $f_{i,\sigma}=0$ or 1. Within the short-range approximation [Eq. (1)], the contribution of the residual interactions to the ground state can be written in first-order perturbation theory as

$$\delta E^{\rm RI} = \frac{F_0^a \Delta}{2}\sum_{i,j} f_{i,(+)} f_{j,(-)} M_{ij}, \tag{3}$$

where Δ is the mean single-particle level spacing in the neighborhood of the Fermi surface. M_{ij} is given by

$$M_{ij} = \mathcal{A}\int d\mathbf{r} |\psi_i(\mathbf{r})|^2 |\psi_j(\mathbf{r})|^2, \tag{4}$$

where $\mathcal{A}$ is the area of the billiard. With this definition, the $\{M_{ij}\}$ are dimensionless quantities with a mean value expected to be roughly equal to unity for $i \neq j$ and to three for $i=j$. These expectations would apply to uncorrelated Gaussian random amplitudes assuming time-reversal invariance holds; ahead more precise results are derived.

Of main interest is how the value of $\delta E^{\rm RI}$ changes when a particle is promoted from one orbital to another (as opposed to the variations in the residual energy as particles are added into the system). Consider that the ground state of the noninteracting N-particle system is such that the levels below the Fermi energy are doubly occupied except for the last level i_F, which may be singly or doubly occupied depending on the parity of N. Promoting a particle from the orbital i_F to i_F+1 has a one-particle energy cost $(E_{i_F+1}-E_{i_F})$. If however this is compensated by the corresponding difference in residual energy, the ground-state occupation numbers $f_{i,(\pm)}$ will be modified by the interactions, yielding in some circumstances nontrivial, i.e., different from 0 or 1/2, ground-state spins. Imagining $\{f_{i,(+)} M_{ij} f_{j,(-)}\}$ in the form of a (square or nearly square) symmetric matrix, shifting an occupancy from one level to another, subtracts the column or row being vacated, and adds a column or row to the newly occupied orbital (row or column depends on the spins of the removed and added particles). Apart from a couple individual M_{ij}'s

near the diagonal, the difference in the residual interaction can therefore be expressed in terms of the difference of two sums of the form

$$\mathcal{S}_i = \sum_{j=1}^{i} M_{ij}. \tag{5}$$

As the $\{M_{ij}\}$ are positive definite, $\mathcal{S}_i$ has a locally defined increasing-with-index positive mean. However, because one column or row is added and another subtracted, their means largely cancel, and thus the mean $\mathcal{S}_i$ behavior cannot be involved in altering the ground-state occupancies of the single-particle levels defined by $U_{\text{conf}}(\mathbf{r})$. (The mean of the few individual M_{ij}'s near the diagonal not included in $\mathcal{S}_i$ might though.) However, if the fluctuations of $\mathcal{S}_i$ or $\{M_{ij}\}$ are sufficiently large, they have the potential to alter the nature of the ground state. Thus, statistical measures based on the properties of the $\mathcal{S}_i$ are of fundamental interest, in particular their mean values and fluctuations.

The $\mathcal{S}_i$ have the unusual character that they are integrated over space and involve a sum over eigenenergies. Their investigation thus requires two basic ingredients. With the definition

$$N(\mathbf{r};E) \equiv \int_0^E dE' n(\mathbf{r};E') = \sum_{i=1}^{\infty} |\Psi_i(\mathbf{r})|^2 \theta(E - E_i). \tag{6}$$

$\mathcal{S}_i$ can be expressed as

$$\mathcal{S}_i = \mathcal{A} \int d\mathbf{r} |\Psi_i(\mathbf{r})|^2 \sum_{j \le i} |\Psi_j(\mathbf{r})|^2 = \mathcal{A} \int d\mathbf{r} |\Psi_i(\mathbf{r})|^2 N(\mathbf{r};E_i^+), \tag{7}$$

with the understanding that $E_i < E_i^+ < E_{i+1}$ (and assuming for simplicity that there are no degeneracies). One of the two required ingredients is the behavior of $N(\mathbf{r};E)$. As it results from a summation over the absolute square of eigenstates up to a certain energy, it is dominated by a secular behavior; see Fig. 13 in Ref. [29], for example. The secular component $N_{\text{sec}}(\mathbf{r};E)$ emerges from an energy smoothing which, although local, is also necessarily broader than the Thouless energy [30]; ahead the notation $\langle\cdot\rangle$ is introduced to denote this averaging. This energy smoothing implies that only dynamics on a time scale shorter than the shortest periodic orbit is relevant, and thus this decomposition is independent of whether the system dynamics is regular, fully chaotic, or has some other character. $N_{\text{sec}}(\mathbf{r};E)$ has been shown to be given by an excellent semiclassical (asymptotic) approximation [29,31],

$$N_{\text{sec}}(\mathbf{r};E) = \frac{N_W(E)}{\mathcal{A}} \left[1 \pm \frac{J_1(2kx)}{kx} \right], \tag{8}$$

where the coordinate x is defined locally as the perpendicular distance from the boundary, k is the magnitude of the wave vector at energy E, and the + sign is for Neumann boundary conditions and the − sign is for Dirichlet boundary conditions. Here $N_W(E)$ refers to just the leading term of the Weyl formula, $N_W(E) = \frac{m\mathcal{A}}{2\pi\hbar^2} E$. The validity is governed by $kL \gg 1$, where L is a length scale, specified ahead in the paper, but which necessarily must be shorter than the width of the system. Away from the boundary, the secular behavior approaches an overall constant. However, the existence of boundary conditions and a minimum wavelength scale combine to create persistent oscillations (Friedel oscillations), which are maximal near the boundary and which fade away toward the interior of the billiard. The negative sign of the Bessel function for Dirichlet boundary conditions respects the vanishing of eigenfunctions at the boundary as it must. Note that just as the critical portion of the density of states can be expressed as a series with volume, boundary, curvature, and oscillatory components, the same is true of $N(\mathbf{r};E)$. The above expression does not include the curvature components and must therefore be missing at least part of the $O([kL]^{-2})$ corrections.

As noted $N_{\text{sec}}(\mathbf{r};E)$ is a smooth function of the parameter E, but $\mathcal{S}_i$ actually involves $N_{\text{sec}}(\mathbf{r};E_i^+)$, which changes abruptly at the points where the energy surpasses each eigenvalue (i.e., is a function of i). The former quantity does not have a monotonous dependence in the number of particles i since E_i contains the Gutzwiller corrections from periodic orbit theory [27,28] that determine the precise positions of the levels. We therefore consider instead the slightly modified and properly normalized decomposition;

$$N(\mathbf{r};E_i^+) = N_{\text{sec}}(\mathbf{r};E_i^+) + \delta N(\mathbf{r};E_i^+),$$

$$N_{\text{sec}}(\mathbf{r};E_i^+) \approx \frac{i}{\mathcal{A}\left(1 \pm \frac{\mathcal{L}}{k_i \mathcal{A}}\right)} \left[1 \pm \frac{J_1(2k_i r)}{k_i r} \right], \tag{9}$$

where the $\mathcal{L}$ is the billiard perimeter and not to be confused with length scale L mentioned above. This decomposition has the further advantage that the fluctuations $\delta N(\mathbf{r};E_i^+)$ not contained in the secular behavior average to zero when integrated over space. In this way, density of states oscillations, which are not of interest here, do not get intertwined with the fluctuations that are the focus of this study. To the order of corrections incorporated in Eq. (9), k_i can equally be defined as $\sqrt{2mE_i}/\hbar$ or as the mean value obtained from the Weyl series.

The other main necessary ingredient is the behavior of $|\Psi_i(\mathbf{r})|^2$ which leads to the two principal approaches contained in this paper. One approach is to rely upon a statistical model which uses an ensemble of random plane waves to mimic the properties of chaotic eigenstates [8,9,32], and the other is to use a semiclassical theory building on the work of Bogomolny [33]. We begin with the random plane-wave modeling as it is technically simpler.

III. RANDOM PLANE-WAVE MODELING

The random plane-wave model [8,9,32] has been introduced in which the eigenstates are represented in the absence of any symmetry by a random superposition of plane waves $\Sigma_l a_l \exp(i\mathbf{k}_l \cdot \mathbf{r})$ with wave vectors of fixed modulus $|\mathbf{k}_l| = k_F$ distributed isotropically. Time-reversal invariance may be introduced as a correlation between time-reversed plane waves such that the eigenfunctions are real. Similarly, the presence

of a planar boundary imposes a constraint between the coefficients of plane waves related by a sign change of the normal component of the wave vector $\mathbf{k}_l$. Near a boundary and using a system of coordinates $\mathbf{r}=\hat{\mathbf{x}}+\hat{\mathbf{y}}$, with $\hat{\mathbf{x}}$ and $\hat{\mathbf{y}}$ as the vectors, respectively, perpendicular and parallel to the boundary (of norm x and norm y), eigenfunctions are therefore locally mimicked statistically by a superposition,

$$\psi_i(\mathbf{r}) = \frac{1}{N_{\text{eff}}} \sum_{l=1}^{N_{\text{eff}}} a_l \mathbf{cs}(\mathbf{k}_l \cdot \hat{\mathbf{x}}) \cos(\mathbf{k}_l \cdot \hat{\mathbf{y}} + \varphi_l) \tag{10}$$

where $\mathbf{cs}(\cdot) \overset{\text{def}}{=} \sin(\cdot)$ for Dirichlet boundary conditions and $\cos(\cdot)$ for Neumann boundary conditions [34]. The phase angle φ_l, the real amplitude a_l, and the orientation of the wave vector $\mathbf{k}_l$ are all chosen randomly. The amplitudes a_l are zero-centered independent Gaussian random variables with $\langle a_l a_{l'} \rangle = \delta_{ll'} \sigma^2$.

To complete the model, it is necessary to determine the variance σ^2 which is fixed by the normalization of the wave functions. Here this constraint is imposed only on average, rather than for each individual state. *A priori*, proceeding in this way might be expected to miss weak correlations between the eigenfunctions. The question is whether one should expect them to be insignificant. In principle, the answer is yes but only if local properties of the eigenfunctions are being considered and the effective dimensionality is large as it would be for $k_F L \gg 1$, where k_F is the Fermi wave vector. This issue is further discussed in the semiclassical theory of Sec. IV ahead.

Using the random plane-wave representation Eq. (10) we have

$$|\psi_i(\mathbf{r})|^2 = \frac{1}{N_{\text{eff}}^2} \sum_{l,l'=1}^{N_{\text{eff}}} a_l a_{l'} \mathbf{cs}(\mathbf{k}_l \cdot \hat{\mathbf{x}}) \mathbf{cs}(\mathbf{k}_{l'} \cdot \hat{\mathbf{x}}) \cos(\mathbf{k}_l \cdot \hat{\mathbf{y}} + \varphi_l) \cos(\mathbf{k}_{l'} \cdot \hat{\mathbf{y}} + \varphi_{l'}), \tag{11}$$

whose expectation value is given by

$$\begin{aligned} \langle |\psi_i(\mathbf{r})|^2 \rangle &= \frac{\sigma^2}{4N_{\text{eff}}^2} \sum_{l=1}^{N_{\text{eff}}} [1 \pm \cos(2\mathbf{k}_l \cdot \hat{\mathbf{x}})] \\ &= \frac{\sigma^2}{4N_{\text{eff}}} \left[1 \pm \frac{1}{2\pi} \int_0^{2\pi} \mathrm{d}\theta \cos(2k_F x \cos\theta) \right] \\ &= \frac{\sigma^2}{4N_{\text{eff}}} [1 \pm J_0(2k_F x)], \end{aligned} \tag{12}$$

where we follow the convention that the upper sign refers to Neumann boundary conditions and the lower sign to Dirichlet boundary conditions, respectively. The ensemble transformation $\frac{1}{N_{\text{eff}}} \Sigma_l \to \frac{1}{2\pi} \int_0^{2\pi} d\theta_l$ has been employed to simplify the calculation. Above, the norms of the wave vectors, equal to k_i, are assumed at or near enough the Fermi surface that they can be denoted by k_F. Integrating over the area of the billiard to fix the normalization gives

$$\begin{aligned} 1 = \int \mathrm{d}\mathbf{r} \langle |\psi_i(\mathbf{r})|^2 \rangle &= \frac{\sigma^2}{4N_{\text{eff}}} \left[\mathcal{A} \pm \mathcal{L} \int_0^\infty \mathrm{d}r J_0(2k_F x) \right] \\ &= \frac{\mathcal{A}\sigma^2}{4N_{\text{eff}}} \left(1 \pm \frac{\mathcal{L}}{2k_F \mathcal{A}} \right), \end{aligned} \tag{13}$$

which fixes the variance σ^2 to next to leading order in $k_F L$.

A. Average properties

The first step in calculating the average behavior of $\mathcal{S}_i$ is to isolate its secular and fluctuating behavior. The model above implies

$$\mathcal{A} \langle |\psi_i(\mathbf{r})|^2 \rangle = \frac{1}{\left(1 \pm \frac{\mathcal{L}}{2k_F \mathcal{A}} \right)} [1 \pm J_0(2k_F x)], \tag{14}$$

and that is consistent with $N_{\text{sec}}(\mathbf{r}; E_i^+)$, i.e., the Friedel oscillation contributions to $N(\mathbf{r}; E_i^+)$. This form applies more generally than the random plane-wave model. Just as $N_{\text{sec}}(\mathbf{r}; E_i^+)$ is independent of system dynamics, so also is this result for the same reasons. For example, it would emerge for integrable systems as well assuming the averaging is over energy intervals greater than the Thouless energy. Finally, note that from the correction to unity of the leading constant in this expression, one sees that if the boundary conditions are Dirichlet, the local mean behavior of $\langle |\psi_i(\mathbf{r})|^2 \rangle$ well into the interior is slightly elevated above $1/\mathcal{A}$ to compensate for the reduced density near the boundary and just the opposite for Neumann boundary conditions.

Let

$$\begin{aligned} \epsilon_i(\mathbf{r}) &= \mathcal{A} |\psi_i(\mathbf{r})|^2 - 1 \\ &= \mathcal{A} \langle |\psi_i(\mathbf{r})|^2 \rangle - 1 + \mathcal{A}[|\psi_i(\mathbf{r})|^2 - \langle |\psi_i(\mathbf{r})|^2 \rangle] \\ &= \pm \frac{1}{\left(1 \pm \frac{\mathcal{L}}{2k_F \mathcal{A}} \right)} \left[J_0(2k_F x) - \frac{\mathcal{L}}{2k_F \mathcal{A}} \right] \\ &\quad + \mathcal{A}[|\psi_i(\mathbf{r})|^2 - \langle |\psi_i(\mathbf{r})|^2 \rangle]. \end{aligned} \tag{15}$$

Under spatial integration, $\epsilon_i(\mathbf{r})$ as well as both halves of the second expression above each separately vanish, whereas only the second half of the expression is affected by taking the expectation value and in that case it vanishes. Ahead, this decomposition simplifies the discussion of the fluctuations.

Returning to the calculation of $\mathcal{S}_i$, substituting the relations from Eqs. (9) and (15), integrating the constant terms, and dropping second-order terms gives

$$\mathcal{S}_i = i \pm \frac{i}{\mathcal{A}} \int d\mathbf{r} \frac{J_1(2k_F x)}{k_F x} \epsilon_i(\mathbf{r}), \tag{16}$$

and therefore

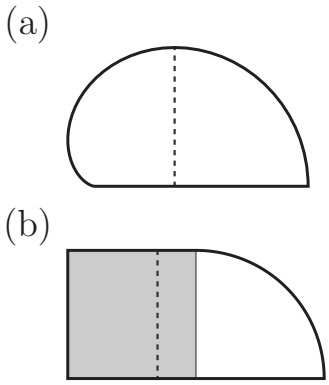

FIG. 1. Drawing of the desymmetrized cardioid and stadium billiard boundaries. The dashed lines illustrate the paths of the shortest periodic orbits for each system. Whereas this orbit is isolated in the cardioid billiard, in the stadium billiard it is a member of a continuous one-parameter family of identical orbits, indicated by the gray-shaded rectangular region.

$$\langle \mathcal{S}_i \rangle = i \pm \frac{i}{\mathcal{A}} \int d\mathbf{r} \frac{J_1(2k_F x)}{k_F x} \langle \epsilon_i(\mathbf{r}) \rangle$$
$$= i + \frac{i}{\mathcal{A}} \int d\mathbf{r} \frac{J_1(2k_F x)}{k_F x} J_0(2k_F x)$$
$$= i\left(1 + \frac{2\mathcal{L}}{\pi k_F \mathcal{A}}\right), \tag{17}$$

where we choose $k_F = \sqrt{2mE_i}/\hbar$. Note the first correction is independent of whether the boundary conditions are Neumann or Dirichlet (see Appendix A for the calculation of second-order terms not related to curvature and discontinuities in the boundary). We stress furthermore that Eq. (17) is applicable independently of the nature of the dynamics, and in particular apply equally well to integrable and chaotic systems. A simple semiclassical proof of this will be given in Sec. IV.

The well-known chaotic cardioid [35–37] and stadium billiards [38–40] are highly suited to illustrating the precision of this relation. The two symmetry-reduced billiard boundaries are illustrated in Fig. 1 along with their shortest periodic orbits to which we return ahead in the discussion of the Fourier transform of the fluctuations.

Comparison to Eq. (17) is shown with a computation of $\mathcal{S}_i$ using the first 2000 odd-parity eigenstates of the cardioid billiard and the same number of even-even eigenstates of the stadium billiard; the latter calculation tests the effects of Neumann boundary conditions. Figure 2 plots the differences, $\mathcal{S}_i - \langle \mathcal{S}_i \rangle$, versus the state index for both billiards. As often happens with semiclassical approximations, even though the result is asymptotic, it is valid right down to either ground state. Note that the second-order corrections have not been included in the secular behavior equations [Eqs. (9) and (14)], and so it is seen that the cardioid results are not centered on zero but on a constant somewhere nearby. The same is also true for the stadium, except that the mean constant was subtracted in order to compare with the solid line predictions from Sec. V B ahead.

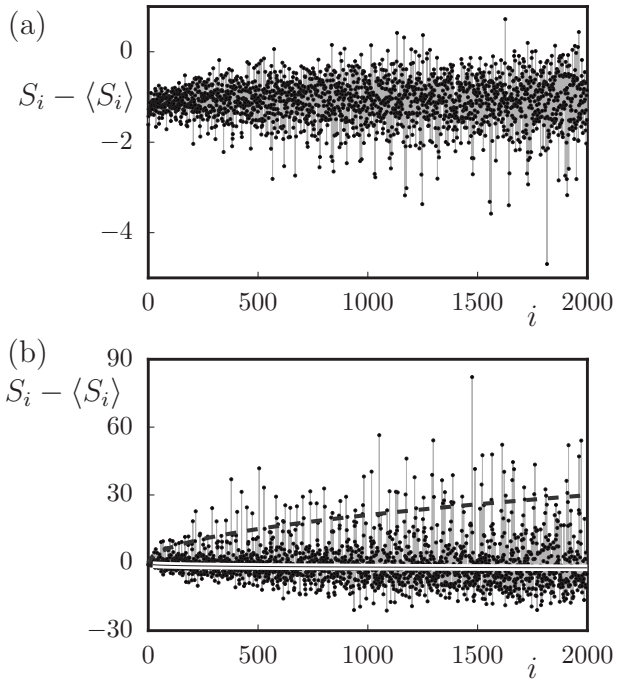

FIG. 2. Comparison of $\mathcal{S}_i$ and the approximation given in the last line of Eq. (17). The difference $\mathcal{S}_i - \langle \mathcal{S}_i \rangle$ is plotted versus the eigenstate number i. In (a), the results for the odd-parity eigenstates of the cardioid billiard using Dirichlet boundary conditions are shown. In (b), the same results for the even-even eigenstates of the stadium billiard with Dirichlet boundary conditions are shown, except that the mean overall constant term has been numerically subtracted. Note the significant increase in the scale of the fluctuations about the mean for the stadium billiard. Ahead in Sec. V B, a rudimentary theory is given for bouncing ball modes that leads to Eqs. (75) and (76) shown as the dashed and solid lines, respectively, in (b).

B. Fluctuations

Consider now the fluctuations of $\mathcal{S}_i$. The quantity that actually sets the scale for the fluctuations in the residual interaction energy is, as discussed in the introduction, approximately the variance $\mathrm{Var}[\mathcal{S}_i - \mathcal{S}_j]$. It is understood that (i,j) do not differ by more than some small integer. More specifically, the interest is in computing this quantity to the leading order in the semiclassical parameter $(k_F L)$.

Using Eq. (7) along with the decomposition into a secular and fluctuating part of $N(\mathbf{r}, E_i^+)$ given by Eq. (9), results in $\mathcal{S}_i$ being written as the sum of two independent terms. The second one, $\mathcal{A}\int d\mathbf{r} |\Psi_i(\mathbf{r})|^2 \delta N(\mathbf{r}; E_i^+)$, has been considered in [20,22] within the random plane-wave approximation. It has a variance scaling as $\log(k_F L)/(k_F L)$, which is of lower order than the leading behavior of $\mathrm{Var}[\mathcal{S}_i]$ calculated ahead. Although, the second term is potentially of physical interest (see Sec. VI), the focus here is on developing the theory that gets the leading term analytically. Applying Eq. (15) and dropping all the lower corrections gives for the covariance between $\mathcal{S}_i$ and $\mathcal{S}_j$

$$\mathrm{Covar}(\mathcal{S}_i\mathcal{S}_j) = \frac{ij}{\mathcal{A}^2}\int d\mathbf{r}_1 \int d\mathbf{r}_2 \frac{J_1(2k_F x_1)}{k_F x_1}\frac{J_1(2k_F x_2)}{k_F x_2} \times[\langle \epsilon_i(\mathbf{r}_1)\epsilon_j(\mathbf{r}_2)\rangle - \langle \epsilon_i(\mathbf{r}_1)\rangle\langle \epsilon_j(\mathbf{r}_2)\rangle]. \quad (18)$$

As before, x and y are the coordinates perpendicular and parallel to the boundary. Not surprisingly, since eigenstate-to-eigenstate correlations are not included in random plane-wave modeling,

$$\langle \epsilon_i(\mathbf{r}_1)\epsilon_j(\mathbf{r}_2)\rangle - \langle \epsilon_i(\mathbf{r}_1)\rangle\langle \epsilon_j(\mathbf{r}_2)\rangle = \delta_{ij}[\langle \epsilon_i(\mathbf{r}_1)\epsilon_i(\mathbf{r}_2)\rangle - \langle \epsilon_i(\mathbf{r}_1)\rangle\langle \epsilon_i(\mathbf{r}_2)\rangle], \quad (19)$$

and thus, $\mathrm{Var}[\mathcal{S}_i - \mathcal{S}_j] = 2\mathrm{Var}[\mathcal{S}_i]$.

Performing a little more algebra gives

$$\langle \epsilon_i(\mathbf{r}_1)\epsilon_i(\mathbf{r}_2)\rangle - \langle \epsilon_i(\mathbf{r}_1)\rangle\langle \epsilon_i(\mathbf{r}_2)\rangle = \mathcal{A}^2[\langle |\psi_i(\mathbf{r}_1)|^2|\psi_i(\mathbf{r}_2)|^2\rangle - \langle |\psi_i(\mathbf{r}_1)|^2\rangle\langle |\psi_i(\mathbf{r}_2)|^2\rangle], \quad (20)$$

where Eq. (10) is applied to evaluate the right-hand side (rhs) of this equation. Each resulting term has a product of four Gaussian random coefficients. The fluctuations are thus given by pairwise correlating coefficients such that

$$\langle a_l a_{l'} a_m a_{m'}\rangle = \langle a_l a_{l'}\rangle\langle a_m a_{m'}\rangle + \langle a_l a_m\rangle\langle a_{l'} a_{m'}\rangle + \langle a_l a_{m'}\rangle\langle a_{l'} a_m\rangle = \sigma^4(\delta_{ll'}\delta_{mm'} + \delta_{lm}\delta_{l'm'} + \delta_{lm'}\delta_{l'm}), \quad (21)$$

where (l,l') are linked to the first coordinate, $\mathbf{r}_1$, and (m,m') are linked to the second coordinate, $\mathbf{r}_2$. The first term, which correlates the wave functions taken at the same position just reproduces the mean $\langle |\psi_i(\mathbf{r}_1)|^2\rangle\langle |\psi_i(\mathbf{r}_2)|^2\rangle$ and cancels from Eq. (20). The two remaining terms give the same contribution, which can be understood as a consequence of time-reversal invariance. Only one of those terms would be nonzero for a time-reversal noninvariant system, and the result for the variance of $\mathcal{S}_i$ would just be divided by 2 in that case.

Therefore, together with averaging over (φ_l, φ_2), the variance is

$$\mathrm{Var}[\mathcal{S}_i] = \frac{8i^2}{\mathcal{A}^2}\frac{1}{N_{\mathrm{eff}}^2}\sum_{l,m=1}^{N_{\mathrm{eff}}}\int d\mathbf{r}_1 d\mathbf{r}_2 \frac{J_1(2k_F x_1)}{k_F x_1}\frac{J_1(2k_F x_2)}{k_F x_2}\mathbf{cs}(\mathbf{k}_l\cdot\mathbf{x}_1)\mathbf{cs}(\mathbf{k}_l\cdot\mathbf{x}_2)\mathbf{cs}(\mathbf{k}_m\cdot\mathbf{x}_1)\mathbf{cs}(\mathbf{k}_m\cdot\mathbf{x}_2)\cos[\mathbf{k}_l\cdot(\mathbf{y}_1-\mathbf{y}_2)] \times\cos[\mathbf{k}_m\cdot(\mathbf{y}_1-\mathbf{y}_2)]. \quad (22)$$

Reflection of either of the vectors $(\mathbf{k}_l, \mathbf{k}_m)$ leaves the integrand unchanged. Thus, $\cos[\mathbf{k}_l\cdot(\mathbf{y}_1-\mathbf{y}_2)]\cos[\mathbf{k}_m\cdot(\mathbf{y}_1-\mathbf{y}_2)]$ is equivalent to $\exp[i(\mathbf{k}_l-\mathbf{k}_m)\cdot(\mathbf{y}_1-\mathbf{y}_2)]$ and can be replaced in the integrand. The summations can be replaced by angular integration again as was done in Eq. (12).

For the purpose of understanding the asymptotic limit, one is tempted to extend the limits of integration in these integrals. However, that generates divergences associated with large $\delta y = y_1 - y_2$ and small $\sin(\theta_l - \theta_m)$ (where $\theta_{l,m}$ is the angle between the vector $\mathbf{k}_{l,m}$ and the direction $\hat{x}$). This indicates that over large distances the random plane-wave model as given by Eq. (10) cannot be applied. One way to think of this is to imagine a true eigenstate of some chaotic billiard. Locally, one could project onto the form of Eq. (10) and approximately solve for a set of coefficients $\{a_l\}$ and plane-wave orientations. However, the solution set $\{a_l\}$ would be dependent on the location along the boundary where the projection was performed due to the rotating orientation of the local coordinate system. Even if the Gaussian random modeling were perfectly fine from state to state, as $\mathbf{r}_2$ got further from $\mathbf{r}_1$, the two cross terms in Eq. (21) that generate the variance would progressively decay on a length scale given by the typical dimension L of the system. This is related to the behavior observed for the spatial autocorrelation function; see Fig. 2 of [41]. (Note that the first term, which reproduces the square of the mean, would on the other hand not decay.) Ahead, it is seen that the results depend only logarithmically on this parameter for Neumann boundary conditions and not at all for Dirichlet so that it is not necessary to describe very precisely this decay as long as the proper length scale is introduced.

A Gaussian form $\exp(-\delta y^2/2L^2)$ is convenient and gives

$$\mathrm{Var}[\mathcal{S}_i] = \frac{8i^2}{\pi^2\mathcal{A}^2}\int_{-\pi/2}^{\pi/2} d\theta_l \int_{-\pi/2}^{\pi/2} d\theta_m \times\left[\int_0^\infty dx \frac{J_1(2k_F x)}{k_F x}\mathbf{cs}(k_F x\cos\theta_l)\mathbf{cs}(k_F x\cos\theta_m)\right]^2 \times\mathcal{L}\int_{-\mathcal{L}/2}^{\mathcal{L}/2} d(\delta y) \times\exp\left(-\frac{\delta y^2}{2L^2} + i(\mathbf{k}_l-\mathbf{k}_m)\cdot(\mathbf{y}_1-\mathbf{y}_2)\right). \quad (23)$$

Including the Gaussian cutoff and noting that the dominant contributions come from regions in which $\sin\delta\theta$ is small (with $\delta\theta = \theta_l - \theta_m$), it is possible to approximate $\sin\theta_l - \sin\theta_m \simeq \cos(\bar{\theta})\delta\theta$, with $\bar{\theta} = (\theta_l + \theta_m)/2$. The integrand $\mathcal{I}(\bar{\theta}, \delta\theta)$ becomes

$$\mathcal{I}(\bar{\theta}, \delta\theta) = \sqrt{2\pi}L\mathcal{L}\left[\frac{1 \pm |\sin(\bar{\theta})|}{2k_F}\right]^2 \exp\left[-\frac{(k_F L\cos\bar{\theta}\delta\theta)^2}{2}\right], \quad (24)$$

where the sign − and + correspond to Dirichlet and Neumann boundary conditions, respectively. Performing the integration over the variables $\delta\theta$ and $\bar{\theta}$ yields

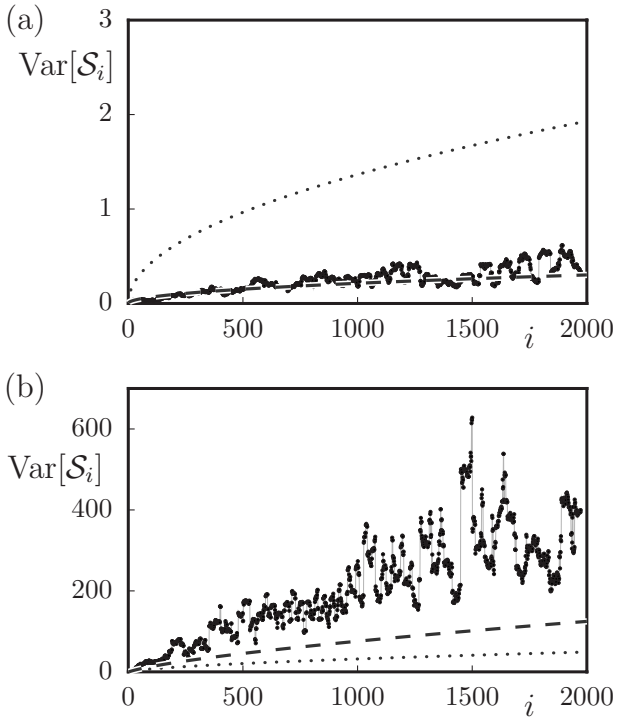

FIG. 3. Variance of $\mathcal{S}_i$ for the cardioid (odd parity only) and quarter stadium (even-even symmetry only) billiards using Dirichlet boundary conditions. In (a), the discrete points are the cardioid billiard results, the dotted line is the result of the random plane-wave model, i.e., Eq. (25), and the long-dashed line is the semiclassical theory, Eqs. (52) and (53), given in Sec. IV A ahead. In (b), the discrete points are the stadium billiard results, the dotted line is the result of the random plane-wave model [Eq. (25)] and the long dashed line is the prediction [Eq. (77)] from the semiquantitative semiclassical theory developed in Sec. V B ahead for the bouncing ball modes.

$$\mathrm{Var}[\mathcal{S}_i] = \frac{k_F \mathcal{L}}{4\pi^3} \langle \lambda^2(\bar{\theta}) \rangle_\theta, \tag{25}$$

where we have introduced the function

$$\lambda(\theta) \overset{\mathrm{def}}{=} \frac{[1 \pm |\sin(\theta)|]}{|\cos(\theta)|}, \tag{26}$$

and the average is defined in terms of the variable $\sin(\theta)$ so that

$$\langle \lambda^2(\theta) \rangle_\theta = \int_0^1 d(\sin\theta) \lambda^2(\theta) = (2 \ln 2 - 1), \quad \text{Dirichlet}, \tag{27}$$

$$= (2 \ln 2 - 1) + 4 \ln \frac{\pi k_F \mathcal{A}}{2\mathcal{L}}, \quad \text{Neumann}. \tag{28}$$

Note that caution must be exercised in evaluating the Neumann case. There the angle $\bar{\theta}$ cannot be allowed to decrease to less than the inverse of $k_F L$ where the cut-off expression becomes invalid. In the absence of other considerations, a very reasonable choice for L is just half the average length between two reflections; see Appendix B. For a two-dimensional (2D) concave billiard, this gives exactly $L = \pi \mathcal{A}/(2\mathcal{L})$, and this value has been substituted into the Neumann form.

Finally, consider the difference between Dirichlet and Neumann boundary conditions. Equations (27) and (28) both roughly imply a $k_F \mathcal{L}$ behavior. The prefactor $\ln(2/\sqrt{e})/2\pi^3 \simeq 0.0031$ is rather small in the first case, whereas for Neumann boundary conditions there is a logarithmic enhancement which can be understood as a (much larger) effective prefactor (a factor 40 larger for $i = 1000$). From the point of view of the calculation, the difference between these two cases can be related to the sign change between $1 - |\sin(\bar{\theta})|$ and $1 + |\sin(\bar{\theta})|$ in Eq. (24), in such a way that whispering gallery modes (for which the corresponding classical orbits have $\bar{\theta} \simeq \pi/2$) are suppressed for Dirichlet boundary conditions, whereas they dominate (because they are less affected by the $\exp[-(k_F L \cos\bar{\theta} \delta\theta)^2/2]$ factor) in the Neumann case. This makes sense since the main source of $\mathcal{S}_i$ fluctuations originates from the wave-function fluctuation probability density $|\psi_i(\mathbf{r})|^2$ in the mean field $\propto \{[1 \pm J_1(2k_F x)]/(k_F x)\}$ generated by the Friedel oscillations of all the other particles below the Fermi energy. Dirichlet boundary conditions however impose that $|\psi_i(\mathbf{r})|^2 \to 0$ as $\mathbf{r}$ approaches the boundary and therefore inhibits this contribution.

Figure 3 illustrates the comparison between the analytical results of the random plane-wave model for the variance [Eq. (25)] for the cardioid and quarter stadium billiards. For the stadium, $k_F \mathcal{L}$ is replaced by $k_F \mathcal{L}_N$, i.e., the length of the straight edges where Neumann boundary conditions are imposed (even-even symmetry class). The theory for the Dirichlet case, cardioid billiard, appears to be roughly a factor 6 too great. In order to understand the discrepancy, the more powerful approach of semiclassical theory is developed in the next section. For the stadium, both Neumann boundary conditions and bouncing ball modes must be considered. This involves additional complications treated in Sec. V B ahead.

IV. SEMICLASSICAL APPROACH

It is important to develop a semiclassical approach. It gives a more powerful theory and sheds some light on the difficulties that the random plane-wave model is having in providing a quantitative description of the $\mathcal{S}_i$ fluctuations. The most immediate conceptual difficulty in getting started is that a treatment of the $\mathcal{S}_i$ implies, through Eqs. (15) and (16), addressing the fluctuations of *individual wave functions*, whereas semiclassical approximations valid for chaotic systems—such as the ones based on the semiclassical Green functions—converge only for quantities smoothed on an energy range containing a significant number of levels. Here, however, this difficulty can be overcome.

For this purpose, let us, following Bogomolny [33], introduce a local energy averaging that is generally much narrower than the Thouless energy

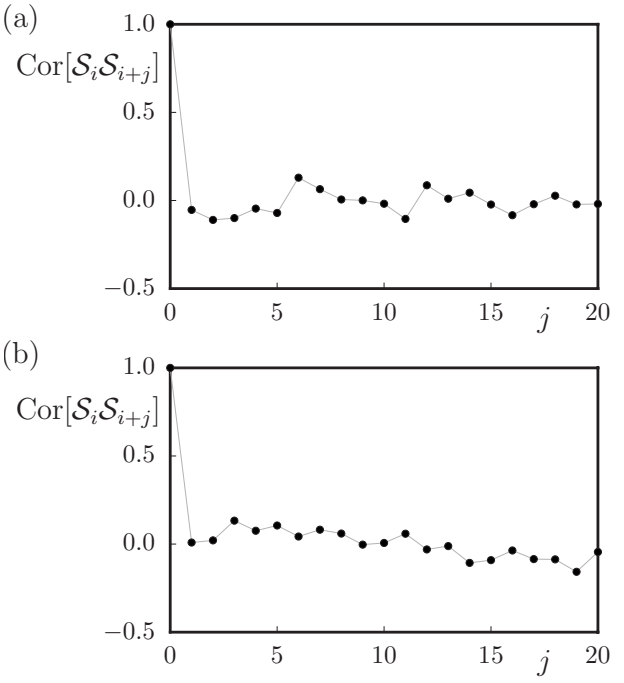

FIG. 4. Correlation function $\mathrm{Cor}[\mathcal{S}_i\mathcal{S}_{i+j}] = \mathrm{Covar}[\mathcal{S}_i\mathcal{S}_{i+j}]/\mathrm{Var}[\mathcal{S}_i]$ for the cardioid and stadium billiard examples. In both cases the correlation function (or covariance) of the billiard is consistent with zero to within sample size fluctuations as assumed in the random plane-wave model and as implied by the semiclassical theory ahead leading to Eq. (51).

$$\overline{\mathcal{S}}_{\Delta N} \overset{\text{def}}{=} \frac{1}{\Delta N} \sum_{E-\Delta E/2<E_i<E+\Delta E/2} \mathcal{S}_i. \tag{29}$$

The notation $\Delta N \overset{\text{def}}{=} N(E+\frac{\Delta E}{2}) - N(E-\frac{\Delta E}{2})$ represents the number of levels in the energy interval $[E-\frac{\Delta E}{2}, E+\frac{\Delta E}{2}]$. With this notation, the variance is

$$\mathrm{Var}[\overline{\mathcal{S}}_{\Delta N}] \overset{\text{def}}{=} \langle (\overline{\mathcal{S}}_{\Delta N} - \langle \mathcal{S} \rangle)^2 \rangle = \frac{1}{\Delta N}\mathrm{Var}[\mathcal{S}_i] + \frac{\Delta N - 1}{\Delta N}\mathrm{Covar}_{i\neq j}[\mathcal{S}_i\mathcal{S}_j], \tag{30}$$

with $(\langle \mathcal{S} \rangle \overset{\text{def}}{=} \langle \mathcal{S}_i \rangle = \langle \overline{\mathcal{S}}_{\Delta N} \rangle)$. Computing the locally averaged quantity $\overline{\mathcal{S}}_{\Delta N}$, for which convergent semiclassical approximations can be used, it is possible to extract the variance and the covariance of the $\mathcal{S}_i$ from the scaling in ΔN of $\mathrm{Var}[\overline{\mathcal{S}}_{\Delta N}]$. In addition, as expected from the random plane-wave description, the correlations among the $\mathcal{S}_i$ are entirely negligible. This is illustrated in Fig. 4, where the average for the covariance is performed over 400 levels starting from $i=1500$. Both cardioid and stadium billiard exhibit correlations which are within the expected statistical errors for being consistent with zero. It is therefore expected (and actually turns out) that the semiclassical evaluation of $\mathrm{Var}[\overline{\mathcal{S}}_{\Delta N}]$ scales as $1/\Delta N$, and it is possible to interpret the corresponding multiplicative factor as $\mathrm{Var}[\mathcal{S}_i]$.

The remaining task is to evaluate semiclassically the locally smoothed quantity $\overline{\mathcal{S}}_{\Delta N}$. For this purpose, two ingredients are needed, the wave-function probabilities $|\Psi_i(\mathbf{r})|^2$ and the density of particles $N(\mathbf{r},E)$. For the eigenfunctions, a semiclassical orbit summation was given by Bogomolny [33]. It is based on the semiclassical approximation of the retarded Green function (given here for two dimensional systems),

$$G^R(\mathbf{r},\mathbf{r}',E) \simeq \frac{1}{i\hbar}\frac{1}{\sqrt{2i\pi\hbar}} \sum_{\mu:\mathbf{r}\to\mathbf{r}'} \frac{1}{\sqrt{|\dot{x}\dot{x}' m_{12,\mu}|}} \exp\left[\frac{i}{\hbar}S_\mu(\mathbf{r},\mathbf{r}',E) - i\frac{\pi}{2}\eta_\mu\right], \tag{31}$$

where the sum runs over all *closed* (i.e., not necessarily periodic) orbits, with S_μ as the classical action of the μ^{th} orbit, $m_{12,\mu} \equiv \partial r'_\perp / \partial p_\perp$ as the stability matrix element, and η_μ as the appropriate geometric index (primed and unprimed variables correspond, respectively, to the initial and final coordinates). $G^R(\mathbf{r},\mathbf{r},E)$ is related to the local density of states and thus to the eigenfunction probability density via

$$\nu(\mathbf{r},E) \equiv \sum_i |\Psi_i(\mathbf{r})|^2 \delta(E-E_i) = -\frac{1}{\pi}\mathrm{Im}\, G^R(\mathbf{r},\mathbf{r},E). \tag{32}$$

Introducing the density of states $\rho(E) \equiv \Sigma_j \delta(E-E_j)$, we obtain

$$\overline{|\Psi_i(\mathbf{r})|^2}_{\Delta N} = \frac{\overline{\nu(\mathbf{r},E_i^+)}_{\Delta E}}{\overline{\rho(E_i^+)}_{\Delta E}}, \tag{33}$$

where on the rhs the overline notation has the same meaning as previously introduced except that the division is by ΔE instead of ΔN.

In the semiclassical evaluation of $\nu(\mathbf{r},E)$, it is typical to distinguish between the "zero-length" orbit contribution $\nu_W(\mathbf{r}) = m/2\pi\hbar^2$ and the contribution of the remaining orbits, whose lengths remain finite as $\mathbf{r}\to\mathbf{r}'$. Here however, interest is in the fluctuations of the eigenfunctions, and thus of $\nu(\mathbf{r},E)$, near the boundary of the billiard. The orbit responsible for the Friedel oscillations, namely, the one returning to its initial location immediately after bouncing off the boundary will therefore be extremely short, implying that (i) the corresponding contribution will not be sensitive to local energy averaging and (ii) if $\mathbf{r}$ is at a distance x from the boundary shorter than or of the order of the Fermi wavelength, the semiclassical approximation [Eq. (31)] cannot be applied. On the other hand, assuming x much smaller than the curvature of the boundary, this contribution can be approximated by the exact result valid (in two dimension) for a straight boundary $\nu_{\mathrm{Friedel}}(x) = \pm\nu_W J_0(2k_F x)$. This gives

$$\overline{\nu(\mathbf{r})}_{\Delta E} = \nu_W[1 \pm J_0(2k_F x)] - \frac{1}{\pi}\mathrm{Im}\,\overline{\widetilde{G}_{\mathrm{osc}}(\mathbf{r},\mathbf{r})}_{\Delta E}, \tag{34}$$

valid near the billiard boundary. The tilde on $\widetilde{G}_{\mathrm{osc}}$ indicates that the short orbits giving rise to the Friedel oscillations have been excluded from the semiclassical sum [Eq. (31)].

Similarly, the density of states is split into a smooth component and an oscillatory one. Once the local energy averaging is performed over a range much larger than the mean level spacing, the oscillatory components are small compared with the smooth term. Thus, the density of states can be expanded in the denominator. Addressing still two-dimensional billiard systems for which $\rho_W(E)=\mathcal{A}\nu_W$ gives

$$\mathcal{A}\overline{|\Psi_i(\mathbf{r})|^2}_{\Delta N} = 1 \pm J_0(2k_F x) - \frac{1}{\nu_W}\frac{1}{\pi}\mathrm{Im}\,\overline{\tilde{G}_{\mathrm{osc}}(\mathbf{r},\mathbf{r},E)}_{\Delta E} - \frac{1 \pm J_0(2k_F x)}{\mathcal{A}\nu_W}\overline{\rho_{\mathrm{osc}}(E)}_{\Delta E}. \tag{35}$$

This equation could be thought of as a slight generalization of the result given by Bogomolny [33], with the only difference that the Bessel function $J_0(2k_F x)$ has been introduced to account for the Friedel oscillations (which turn out to be important here); see Appendix C for an improved normalization of this equation.

For ΔE large on the scale of the mean level spacing, but small on the classical scale, the energy smoothing can be performed for each orbit contribution noting that $\partial S_\mu/\partial E=\tau_\mu$, with τ_μ as the time of travel of the orbit, giving

$$\overline{\exp\left(\frac{i}{\hbar}S_\mu\right)}_{\Delta E} = \exp\left(\frac{i}{\hbar}\bar{S}_\mu\right)\mathrm{sinc}\left(\frac{\tau_\mu \Delta E}{2\hbar}\right), \tag{36}$$

with $[\mathrm{sinc}(x) \overset{\mathrm{def}}{=} \sin(x)/x]$. Energy smoothing therefore implies that orbits with periods greater than $\hbar/\Delta E$ are cut off in the semiclassical sums Eqs. (31)–(35).

As a direct (and expected) consequence, if the smoothing takes place on a energy range larger than the Thouless energy, no orbit can contribute to $\overline{\tilde{G}_{\mathrm{osc}}(\mathbf{r},\mathbf{r},E)}_{\Delta E}$ or $\overline{\rho_{\mathrm{osc}}(E)}_{\Delta E}$, and the average wave-function probability reduces to $\mathcal{A}\langle|\Psi_i(\mathbf{r})|^2\rangle = 1 \pm J_0(2k_F x)$. Inserting this equality into Eq. (16) with the definition Eq. (15), we readily obtain the result [Eq. (17)] for the mean value $\langle \mathcal{S}_i \rangle$, but here without any assumption regarding the nature of the dynamics; i.e., it applies equally well for integrable, mixed, or chaotic systems.

A. Chaotic quantized billiards

Up to this point, the nature of the dynamics has played no role in the semiclassical approach. However, beginning here, the approach is specialized to chaotic systems. The oscillating component (a sum over periodic orbits [28]) of the density of states is given by

$$\rho_{\mathrm{osc}}(E) = \frac{1}{\pi\hbar}\sum_{\gamma=\mathrm{periodic\ orbit}}\frac{\tau_\gamma}{|\mathrm{Det}(M_\gamma - 1)|^{1/2}} \times \cos\left(\frac{S_\gamma(E_i^+)}{\hbar} - \eta_\gamma\frac{\pi}{2}\right), \tag{37}$$

where τ_γ is the period of the periodic orbit, M_γ is the monodromy matrix, and η_γ is the appropriate geometric index.

For a two-degree-of-freedom billiard, $\mathcal{A}\overline{|\Psi_i(\mathbf{r})|^2}_{\Delta N} \simeq 1 \pm J_0(2k_F x) + \overline{\epsilon_i^{(1)}(\mathbf{r})}_{\Delta N} + \overline{\epsilon_i^{(2)}(\mathbf{r})}_{\Delta N}$, with

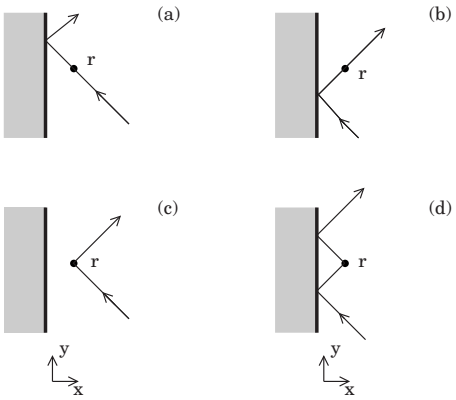

FIG. 5. Sketch of the four orbits which, as $x \to 0$, coalesce into the same [nearly] periodic orbit. The top row corresponds to two (nearly) periodic orbits such that $\mathbf{r}$ lies on the trajectory either (a) just before or (b) just after the bounce off the boundary. The bottom row corresponds to two nonperiodic orbits ($p_x' = -p_x$) such near $\mathbf{r}$ (c) one of them does not touch the boundary and (d) the other one touches twice.

$$\overline{\epsilon_i^{(1)}(\mathbf{r})}_{\Delta N} \approx \frac{2\sqrt{\hbar}}{m}\mathrm{Im}\frac{i}{\sqrt{2\pi i}}\sum_{\mu=\mathrm{closedorbit}}\frac{1}{\sqrt{|\dot{x}_\mu \dot{x}_\mu' m_{12,\mu}|}} \times \overline{\exp\left[i\frac{S_\mu(\mathbf{r},\mathbf{r})}{\hbar} - i\nu_\mu\frac{\pi}{2}\right]}_{\Delta E}, \tag{38}$$

$$\overline{\epsilon_i^{(2)}(\mathbf{r})}_{\Delta N} \approx \frac{2\hbar}{m\mathcal{A}}[1 \pm J_0(2k_F x)]\sum_{\gamma=\mathrm{periodic\ orbit}} \times \frac{\tau_\gamma}{|\mathrm{Det}(M_\gamma - 1)|^{1/2}}\overline{\cos\left(\frac{S_\gamma}{\hbar} - \bar{\nu}_\gamma\frac{\pi}{2}\right)}_{\Delta E}. \tag{39}$$

Note that the μ-orbit sum here includes all returning orbits, not just those in the neighborhood of a complete periodic orbit.

One might also be tempted to use the same expressions integrated over energy to deduce a similar expression for $N(\mathbf{r};E_i^+)$. However, the energy integral generates a factor $\sim\hbar/\tau_i E$ for the oscillating contribution of an orbit of period τ_i, and therefore the oscillating terms obtained in this way would be of lower order in $\hbar$ than those generated by $|\Psi_i(\mathbf{r})|^2$. In leading order, it is therefore only necessary to keep the terms of $N(\mathbf{r};E_i^+)$ associated with the Friedel oscillations, i.e., begin with Eq. (16) directly and drop further subleading terms. Thus, $\mathcal{S}_i = \bar{\mathcal{S}} \pm [\mathcal{S}_{i,\mathrm{osc}}^{(1)} + \mathcal{S}_{i,\mathrm{osc}}^{(2)}]$, where

$$\mathcal{S}_{i,\mathrm{osc}}^{(\alpha)} = \frac{i}{\mathcal{A}}\int d\mathbf{r}\frac{J_1(2k_F x)}{(k_F x)}\epsilon_i^{(\alpha)}(\mathbf{r}) \tag{40}$$

($\alpha = 1,2$). Here, two remarks are in order. First, because only the very short orbit contribution [i.e., the term proportional to $J_1(2k_F x)/(k_F x)$] is kept for $N(\mathbf{r},E)$, it is not sensitive to the local energy average and can be taken out of the bracket. Second, note that the main contribution to the integral over space in the rhs of Eq. (40) is restricted to the vicinity of the boundary. As before we can unambiguously use a system of coordinates $\mathbf{r}=(x,y)$, with x perpendicular and y parallel to

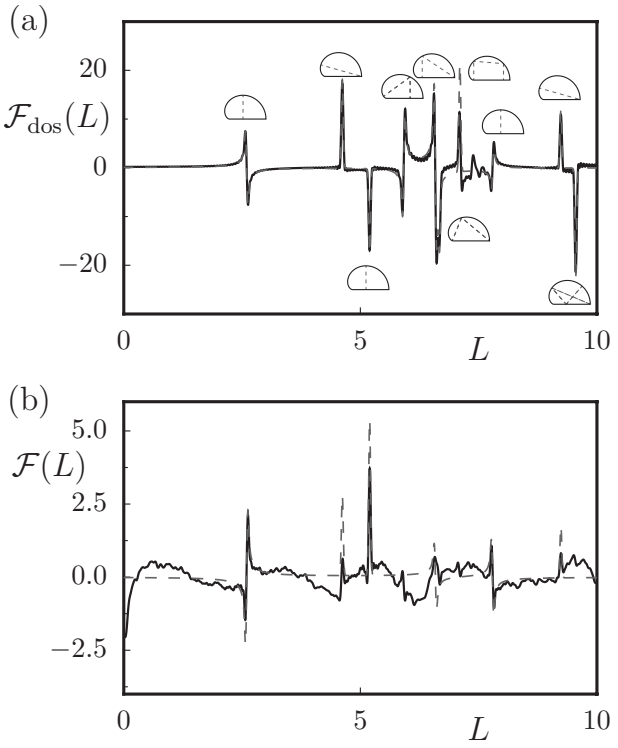

FIG. 6. Fourier transform of the density of states and $\mathcal{S}_i-\langle\mathcal{S}_i\rangle$ of the cardioid billiard using Dirichlet boundary conditions. In (a), the solid line is for the density of states using the first 2000 odd-parity levels of the cardioid billiard. The dashed line is for the density of states using the corresponding form of the Gutzwiller trace formula. In (b), the solid line is the Fourier transform of $\mathcal{S}_i-\langle\mathcal{S}_i\rangle$ for the first 2000 $\mathcal{S}_i$ and the dashed line is the result of Eq. (45) calculated for the shortest periodic orbits as the one shown in Fig. 1 and the insets (along with their retracings). The agreement is quite good.

the boundary. To compute $\mathcal{S}^{(1)}_{i,\rm osc}$, insert Eq. (39) into Eq. (40). A stationary phase condition has to be imposed in the y direction but not in the x direction since the effective range of interaction is not large even on the scale of the Fermi wavelength. As a consequence, the dominant contributions of the integration involved in Eq. (40) come from the neighborhood of trajectories such that $p'_y=p_y$ [where the primed (unprimed) correspond to initial (final) momentum] but for which the initial and final x momenta may differ. Energy conservation however imposes $p'_x=\pm p_x$. As illustrated in Fig. 5, these trajectories can be associated to a cluster of four orbits which, as $x\to 0$, converges smoothly toward the same nearly periodic orbit (or fixed point of the boundary Poincaré map): (i) two nearly periodic orbits such that $\mathbf{r}$ lies on the trajectory just before or just after bouncing off the boundary and (ii) two nonperiodic ones ($p'_x=-p_x$) either touching the boundary twice or not at all near $\mathbf{r}$.

Denoting $S_{l_0}(0,y)$ the action of the nearly periodic orbit to which all of these orbits converge as $x\to 0$, leads to $S_l(x,y)=S_{l_0}(0,y)+\delta S_l(x,y)$, where $\delta S_l\simeq(p'_x-p_x)x$, which vanishes for the two periodic orbits and gives $\pm 2|p|x\cos\theta_l$, with θ_l as the angle of incidence of the periodic orbit on the boundary, for the two nonperiodic ones. Noting that $\exp(i2kx\cos\theta_l)+\exp(-i2kx\cos\theta_l)\pm 2=4\mathbf{cs}^2(kx\cos\theta_l)^2$ gives

$$\overline{\mathcal{S}^{(1)}_{i,\rm osc\Delta N}}=\frac{8\sqrt{\hbar}}{m\mathcal{A}}\sum_{l=\text{fixed point}}\text{sinc}\left(\frac{\tau_l\Delta E}{2\hbar}\right)\times\int_0^\infty dx\frac{J_1(2kx)}{kx}\mathbf{cs}^2(kx\cos\theta_l)\times\text{Im}\frac{i}{\sqrt{2\pi i}}\int_{-\mathcal{L}/2}^{\mathcal{L}/2}dy\frac{1}{\sqrt{|\dot{x}_l||\dot{x}'_l||m_{12,l}|}}\times\exp\left[i\frac{S_l[(0,y),(0,y);E]}{\hbar}-i\nu_l\frac{\pi}{2}\right],\quad(41)$$

where the sum runs over all the fixed points of the boundary Poincaré section. As in the previous section $\int_0^\infty dx\frac{J_1(2kx)}{kx}\mathbf{cs}^2(kx\cos\theta_l)=[1\pm|\sin\theta_l|]/2k$. Furthermore, the integral in the parallel direction can be performed in a very similar way as in the derivation of the Gutzwiller trace formula. Using the fact that near the periodic point $(0,y_l)$

$$S_l\{[(0,y_l+\delta y),(0,y_l+\delta y);E]\}=S_l(E)+\frac{\text{Det}(M_l-1)}{2m_{12,l}}\delta y^2\quad(42)$$

and $|\dot{x}_l|=|\dot{x}'_l|=v_F|\cos\theta_l|$, we get

$$\overline{\mathcal{S}^{(1)}_{i,\rm osc\Delta N}}=\frac{4i}{\mathcal{A}k_F^2}\sum_{l=\text{fixed point}}\lambda(\theta_l)\times\frac{\cos\left[\frac{S_l(E)}{\hbar}-\bar{\nu}_l\frac{\pi}{2}\right]}{\sqrt{|\text{Det}(M_l-1)|}}\text{sinc}\left(\frac{\tau_l\Delta E}{2\hbar}\right),\quad(43)$$

with $\lambda(\theta)\overset{\text{def}}{=}[1\pm|\sin\theta|]/|\cos\theta|$ as the same function that was introduced in the random plane-wave approach [cf. Eq. (26)].

The computation of $\overline{\mathcal{S}^{(2)}_{i,\rm osc\Delta N}}$ is even simpler as the only spatial dependence of $\epsilon_i^{(2)}$ arises from the Bessel function $J_0(2k_Fx)$. To facilitate the comparison with Eq. (43), replace the sum over periodic orbits by a sum over fixed points of the Poincaré section, in which case the period τ_γ of the periodic orbit has to be replaced by the average time of flight $\tau_\gamma/n_\gamma=\ell_\gamma/v_Fn_\gamma$ (ℓ_γ and n_γ are, respectively, the total length and total number of bounces of the periodic orbit γ) between two successive bounces on the boundary. Using $\int_0^\infty(du/u)J_1(u)[1\pm J_0(u)]=(1\pm 2/\pi)$ gives

$$\overline{\mathcal{S}^{(2)}_{i,\rm osc\Delta N}}=-\frac{4i}{\mathcal{A}k_F^2}\sum_{l=\text{fixed point}}\frac{\mathcal{L}\ell_l}{2n_l\mathcal{A}}\left(1\pm\frac{2}{\pi}\right)\times\frac{\cos\left[\frac{S_l(E)}{\hbar}-\bar{\nu}_l\frac{\pi}{2}\right]}{\sqrt{|\text{Det}(M_l-1)|}}\text{sinc}\left(\frac{\tau_l\Delta E}{2\hbar}\right),\quad(44)$$

where $n_l\overset{\text{def}}{=}n_{\gamma(l)}$ is the number of bounces of the periodic orbit to which l belongs, and a similar notation is implied for the other parameters. This actually depends only on the periodic

orbit γ and not on the specific periodic point l on γ. The $(2/\pi)$ factor can be traced back to the $J_0(2k_F x)$ term and therefore eventually to the Friedel oscillations of the local density of states.

The two terms can be combined to give

$$\bar{\mathcal{S}}_{\Delta N} - \langle \mathcal{S} \rangle = \pm \frac{4i}{\mathcal{A}k_F^2} \sum_{\gamma=\text{periodic orbit}} \frac{\cos\left[\frac{S_\gamma(E)}{\hbar} - \bar{\nu}_\gamma \frac{\pi}{2}\right]}{\sqrt{|\text{Det}(M_\gamma - 1)|}} \text{sinc}\left(\frac{\tau_\gamma \Delta E}{2\hbar}\right) \times \sum_{l=\text{fixed point of } \gamma} \left[\lambda(\theta_l) - \frac{\mathcal{L}\ell_l}{2\mathcal{A}n_l}\left(1 \pm \frac{2}{\pi}\right)\right]. \tag{45}$$

This form is suitable for performing the calculation of the variance. However, as rederived briefly in Appendix B, note that the mean length per bounce in a billiard is

$$\bar{d} = \frac{\pi \mathcal{A}}{\mathcal{L}}. \tag{46}$$

Also, the density of fixed points is uniform for long orbits in the measure $d \sin\theta$. Averaging with that measure while replacing $\mathcal{L}\ell_l/2\mathcal{A}n_l$ by its mean value $\pi/2$ gives

$$\left\langle \lambda(\theta_l) - \frac{\mathcal{L}\ell_l}{2\mathcal{A}n_l}\left(1 \pm \frac{2}{\pi}\right)\right\rangle_\theta = \frac{1}{2}\int_{-\pi/2}^{\pi/2} d\sin\theta \frac{(1 \pm |\sin\theta_l|)}{|\cos\theta_l|} - \frac{\pi}{2}\left(1 \pm \frac{2}{\pi}\right) = \frac{\pi}{2} \pm 1 - \frac{\pi}{2}\left(1 \pm \frac{2}{\pi}\right) = 0. \tag{47}$$

Thus, the constant $\frac{\mathcal{L}\bar{d}}{2\mathcal{A}}(1 \pm \frac{2}{\pi})$ can be understood as arising from $\bar{\mathcal{S}}^{(2)}_{i,\text{osc}\Delta E}$ (i.e., associated with the density of states) as the angular mean $\langle \lambda(\theta) \rangle_\theta$ of the corresponding term in $\bar{\mathcal{S}}^{(1)}_{i,\text{osc}\Delta E}$.

To compute the variance, it is necessary to square Eq. (45) and average the resulting expression over a large energy range. For two periodic orbits γ and γ', $\langle \cos[\frac{S_\gamma(E)}{\hbar} - \bar{\nu}_\gamma \frac{\pi}{2}] \cos[\frac{S_{\gamma'}(E)}{\hbar} - \bar{\nu}_{\gamma'} \frac{\pi}{2}] \rangle$ equals one-half if γ and γ' are either the same orbit or time-reversal symmetric but zero otherwise, which makes cross terms from different periodic orbits vanish. Note however that it does not eliminate cross terms of the various fixed points for a given orbit since these contributions oscillate with the same frequency. This gives

$$\langle (\bar{\mathcal{S}}_{\Delta N} - \langle \mathcal{S} \rangle)^2 \rangle = \frac{g_s}{2} \frac{16 i^2}{k^4 A^2} \sum_{\text{orbit } \gamma} \frac{1}{|\text{Det}(M_l - 1)|} \text{sinc}^2\left(\frac{\tau_\gamma \Delta E}{2\hbar}\right) \times \sum_{\substack{l,l' \\ \text{fixed point of } \gamma}} \left[\lambda(\theta_l) - \frac{\mathcal{L}\ell_\gamma}{2\mathcal{A}n_\gamma}\left(1 \pm \frac{2}{\pi}\right)\right] \times \left[\lambda(\theta_{l'}) - \frac{\mathcal{L}\ell_\gamma}{2\mathcal{A}n_\gamma}\left(1 \pm \frac{2}{\pi}\right)\right]. \tag{48}$$

For long orbits, which are going to dominate this sum, it is possible to identify ℓ_γ/n_γ with $\bar{d} = \pi\mathcal{A}/\mathcal{L}$, the mean length per bounce in the billiard, and assume that the angles θ_l are uncorrelated and uniformly distributed with the measure $d\sin\theta$. It turns out for the last sum in Eq. (48)

$$\sum_{\substack{l,l' \\ \text{fixed point of } \gamma}} \left[\lambda(\theta_l) - \frac{\mathcal{L}d_\gamma}{2\mathcal{A}n_\gamma}\left(1 \pm \frac{2}{\pi}\right)\right]\left[\lambda(\theta_{l'}) - \frac{\mathcal{L}d_\gamma}{2\mathcal{A}n_\gamma}\left(1 \pm \frac{2}{\pi}\right)\right] \simeq n_\gamma \left\langle \left[\lambda(\theta) - \frac{\mathcal{L}\bar{d}}{2\mathcal{A}}\left(1 \pm \frac{2}{\pi}\right)\right]^2 \right\rangle_\theta + n_\gamma(n_\gamma - 1)\left\langle \left[\lambda(\theta) - \frac{\mathcal{L}\bar{d}}{2\mathcal{A}}\left(1 \pm \frac{2}{\pi}\right)\right] \right\rangle_\theta^2 = n_\gamma \langle (\lambda(\theta) - \langle\lambda\rangle_\theta)^2 \rangle_\theta, \tag{49}$$

where Eq. (47) has been used to cancel the cross terms between different fixed points. Making use of the Hannay–Ozorio de Almeida sum rule [42] in the form

$$\sum_{\substack{\text{fixed points } l \\ \text{with } n \text{ bounces}}} \frac{1}{|\text{Det}(M_l - 1)|} = 1, \tag{50}$$

(where the sum runs over all fixed points belonging to a periodic orbit with n bounces), identifying the period τ of the orbit with $n\bar{d}/v_F$ ($v_F = \hbar k_F/m$ is the Fermi velocity), replacing the sum over the number of bounces by an integral, and making use of Eq. (46) gives

$$\overline{(\langle \mathcal{S} \rangle_{\Delta N} - \overline{\mathcal{S}})^2} = \frac{g_s}{2} \frac{16 i^2}{k^4 A^2} \langle (\lambda(\theta) - \langle \lambda \rangle_\theta)^2 \rangle_\theta \int dn \ \mathrm{sinc}^2 \left(\frac{n \bar{d} \Delta E}{2 \hbar v_F} \right) = \frac{g_s}{2} \frac{k_F \mathcal{L}}{2 \pi^3} \langle (\lambda(\theta) - \langle \lambda \rangle_\theta)^2 \rangle_\theta \frac{1}{\Delta N}. \tag{51}$$

As expected, the variance of $\overline{\mathcal{S}}_{\Delta N}$ is inversely proportional to $\Delta N = \rho_W(E) \Delta E$. Applying Eq. (30), the absence of a term constant with ΔN confirms that, as assumed in the random plane-wave approach, there are at this level of approximation no correlations among the $\mathcal{S}_i$. Thus, the variance of the $\mathcal{S}_i$ are given by

$$\mathrm{Var}(\mathcal{S}_i) = \frac{k_F \mathcal{L}}{2 \pi^3} \times \langle [\lambda(\theta) - \langle \lambda \rangle_\theta]^2 \rangle_\theta, \tag{52}$$

with

$$\langle (\lambda(\theta) - \langle \lambda \rangle_\theta)^2 \rangle_\theta = \begin{cases} (2 \ln 2 - 1) - \left(\frac{\pi}{2} - 1 \right)^2 & \text{Dirichlet} \\ (2 \ln 2 - 1) - \left(\frac{\pi}{2} - 1 \right)^2 + 4 \left(\ln \frac{\pi k_F \mathcal{A}}{2 \mathcal{L}} - \frac{\pi}{2} \right) & \text{Neumann}. \end{cases} \tag{53}$$

B. Periodic orbit spectrum

Beyond the Var$[\mathcal{S}_i]$, which here characterizes the universal (long time) behavior of the system under consideration, the semiclassical treatment developed in the previous subsection provides information on system specific quantities. In particular, it makes it possible to address phenomenon related to shorter time dynamics, and thus quantum mechanically, to longer energy range. For example, Eq. (45) can be used directly to compute the Fourier transform of the $\mathcal{S}_i$. Interestingly, Eq. (45) has a structure very similar to that of the density of states Eq. (37). This gives a simple and striking prediction, namely, that the Fourier transform of the $\mathcal{S}_i$ will display peaks at the same locations and with the same shapes as the Fourier transform of $\rho(E)$ (up to the transformation $i \leftrightarrow E$) and will be simply scaled by factors which depend only on the lengths of the orbits and on their angles of incidences $\{\theta_l\}$ at the various places where they bounce along the boundary. In Fig. 6(a), the Fourier transform of the cardioid billiard density of states is shown in comparison with the Fourier transform of the $\{\mathcal{S}_i\}$ displayed in Fig. 6(b). The peaks are in precisely the same positions and their shapes are similar but the amplitudes differ as expected; as a parenthetical remark, for technical reasons the Fourier transform of the $\{\mathcal{S}_i\}$ uses a slightly different Fourier transform than the density of states (effectively divided by the wave vector), which is denoted by a subscript in the remaining figures, but this has no effect on the overall discussion of the physics involved. In addition, the prediction of Eq. (45) for the shortest periodic orbits and their retracings is shown. The predicted amplitudes for the $\{\mathcal{S}_i\}$ are reasonably close although perhaps slightly too large by 30–50 %. Otherwise, the agreement with Eq. (45) is excellent. The excess in the prediction for short orbits is curious because if the predicted amplitudes for all of the orbits were too large, it should be found that the prediction of the variance is slightly too large instead of a bit too small (say factor of 2) as in this case. We have checked that in fact the predictions for long orbits, which dominate the calculation of the variance of $\{\mathcal{S}_i\}$, are indeed a bit too small, the opposite of the short orbits. Why it has turned out this way for this particular example remains for future consideration.

As a last remark, note that the tendency for long orbits to explore uniformly the phase space implies both that $\sin \theta_l$ is distributed uniformly and that the mean length between bounces ℓ_γ / n_γ for a given orbit γ can be identified with $\bar{d}$, the full system average distance between bounce. This is what made it possible to apply Eq. (47) and to cancel the cross terms between various fixed points of the same orbit in Eq. (49). Had the term proportional to n_γ^2 in Eq. (49) not been zero, it would have given rise to a contribution parametrically larger (in $\hbar$) than the computed one [$\sim (k_F \mathcal{L})^2$ instead of $(k_F \mathcal{L})$]. Short orbits, for which the cancellation of cross terms done in Eq. (49) cannot be applied may therefore have a stronger influence on the fluctuations of the $\mathcal{S}_i$'s than what might be naively expected from Eq. (51).

C. Basic distinctions in the two theoretical approaches

Interestingly enough, the expressions in Eq. (53) are exactly the same results as the random plane-wave approach Eqs. (27) and (28), except for two differences. First, the mean square $\langle \lambda^2(\theta) \rangle_\theta$ has been replaced by the variance of $\lambda(\theta)$, giving now a much better agreement with the billiard results (see Fig. 3). Second there is a factor two difference in the prefactor.

1. Proper normalization

The replacement of the mean square by the variance can be related to the lack of proper normalization of the wave function in the random plane-wave model. Indeed, fluctuations of the local density of states $\nu(\mathbf{r})$ can either imply fluctuations of the wave-function probabilities $|\Psi(\mathbf{r})|^2$, which have to integrate to zero because of the wave-function normalization, or fluctuations of the total density of states for the part which survives the integration over space. The role of the term proportional to $\overline{\rho_{\mathrm{osc}}(E)}_{\Delta E}$ in the right-hand side of

Eq. (35) can therefore be understood as ensuring the normalization of the eigenfunctions. As this term is precisely the one giving rise to the contribution proportional to $\langle\lambda\rangle_\theta^2$, it turns out that in the semiclassical calculation, proper normalization of the eigenfunction is what generates the variance of $\lambda(\theta)$ rather than its mean square. Since the random plane-wave model used here imposes normalization on average rather than for each individual eigenfunction, this contribution is necessarily missing there. A modified version of the random plane-wave model in which normalization is better enforced [43,44] should, however, properly address this issue.

2. Dynamical correlations

The factor two difference in the prefactor (or conversely, the fact that except for this factor 2 and the normalization effect, the random plane wave, and the semiclassical expressions are identical), although less important from a quantitative point of view, is however puzzling enough to deserve further discussion. To focus better on the main point, consider two simplifications of the problem under discussion. First, assume as understood the issue of eigenfunction normalization and consider below only the contribution from the Green function (i.e., ignore density of states fluctuations). Second, consider that the procedure used to extract the variance $\mathrm{Var}[\mathcal{S}_i]$ from the locally smoothed quantity $\overline{\mathcal{S}}_{\Delta N}$ [see Eq. (30)] is equivalent to the effective rule according to which the various quantities under consideration should be smoothed over an energy window of width Δ (so that $\Delta N=1$).

Having this local smoothing in mind and ignoring for the moment the fluctuations of the density of states (i.e., assuming there is exactly one state in each interval δ) gives

$$\overline{\left[\sum_\kappa \Psi_\kappa(\mathbf{r}')\Psi_\kappa^*(\mathbf{r}')\right]}_\Delta = \frac{1}{\Delta}\Psi_\kappa(\mathbf{r}')\Psi_\kappa^*(\mathbf{r}') \tag{54}$$

$$\simeq -\frac{1}{\pi}\mathrm{Im}[G^R(\mathbf{r}',\mathbf{r}',E)]. \tag{55}$$

Close to some reference point $\mathbf{r}$ and not considering yet the proximity of a boundary, this gives for the oscillating part of the wave-function probability

$$\mathcal{A}|\Psi(\mathbf{r}')|^2_{\mathrm{osc}} = -\frac{1}{\pi\nu_W}\left\{\sum_{\mu:\mathbf{r}\to\mathbf{r}} A_\mu \exp[(\mathbf{p}_\mu^f - \mathbf{p}_\mu^i)\mathbf{r}'] + \mathrm{c.c.}\right\}. \tag{56}$$

Above, the sum runs over all closed trajectories μ starting and ending on the reference point $\mathbf{r}$, with initial and final momenta $\mathbf{p}_\mu^i$ and $\mathbf{p}_\mu^f$, time of travel τ_μ, and

$$A_\mu = \frac{1}{i\hbar}\frac{1}{2i\pi\hbar}\frac{1}{\sqrt{|\dot{x}_\mu \dot{x}'_\mu m_{12,\mu}|}}\exp\left[i\frac{S_\mu(\mathbf{r},\mathbf{r})}{\hbar} - i\nu_\mu\frac{\pi}{2}\right]. \tag{57}$$

In the semiclassical calculations of Sec. IV, it is taken into account that as the integration over space is performed, closed trajectories are continuously deformed, and in particular the initial and final momenta $\mathbf{p}_\mu^i$ and $\mathbf{p}_\mu^f$ vary. As a consequence the dominant contributions, which correspond to nearly periodic trajectories (to within a bounce off the billiard boundary in this particular calculation), can be understood as arising from the neighborhood of periodic orbits, leading to the periodic orbit sum [Eq. (43)]. The calculation of the variance is then done using the Hannay–Ozorio de Almeida sum rule [Eq. (50)].

Consider that if the dynamical correlations, i.e., variations in the orbital properties (initial, final momenta $\mathbf{p}_\mu^i$, $\mathbf{p}_\mu^f$, prefactor A_μ, etc.) are neglected, the semiclassical expression for $\Psi^*(\mathbf{r}')\Psi(\mathbf{r}')$ greatly resembles the random plane-wave model. Indeed, if long orbits are dominant:

(i) Initial and final momenta $\mathbf{p}_\mu^i$ and $\mathbf{p}_\mu^f$ are independent and uniformly cover the energy surface, i.e., the model can be taken as a "random pair of plane-waves" model.

(ii) Applying the diagonal approximation in the semiclassical calculation amounts to $\overline{A_\mu^* A_{\mu'}} \propto \delta_{\mu\mu'}$ or if the system is time-reversal invariant μ and μ' are related through time-reversal invariance. Near a boundary, the correlations are included between the trajectories related to one another by a bounce off the boundary.

(iii) Although the A_μ are not Gaussian distributed, the fact that the number of trajectories is extremely large for long orbit makes it possible to use a central limit theorem, implying that only the variance of these quantities are relevant (and that one can as well consider them as Gaussian).

(iv) The variance of the A_μ is constrained by the sum-rule valid for closed orbits (a slightly different rule than the Hannay–Ozorio de Almeida sum rule used for periodic orbits) [45],

$$\sum_\mu |A_\mu|^2 \delta(\tau - \tau_\mu) = \frac{2\pi}{\hbar}\nu_W P_{\mathrm{cl}}(\mathbf{r},\mathbf{r},\tau), \tag{58}$$

where for long orbits in billiards, the probability of return $P_{\mathrm{cl}}(\mathbf{r},\mathbf{r},\tau)$ can be taken uniform and equal to $1/\mathcal{A}$. Properly carrying out the smoothing on the range Δ produce the damping factor $\mathrm{sinc}(\frac{\tau_\mu\Delta}{2\hbar})$ of Eq. (36) so that

$$\sum_\mu |A_\mu|^2 = \frac{2\pi}{\hbar}\frac{\nu_W}{\mathcal{A}}\int_0^\infty \mathrm{sinc}\left(\frac{\tau_\mu\Delta}{2\hbar}\right)dt = 2\pi^2\nu_W^2. \tag{59}$$

Thus, neglecting the spatial variations in the orbits properties which contain dynamical correlations, quite standard semiclassical approximations, namely, the diagonal approximation and the assumption that $P(\mathbf{r},\mathbf{r},\tau)$ is uniform, makes it possible to derive a "pair of random plane-waves" model, not completely identical to the original random plane-wave model but similar in spirit. It can be shown furthermore than computing $\mathrm{Var}[S_i]$ under this model gives exactly the same result as the random plane-wave model.

Indeed, one can compute $\langle\epsilon_i(\mathbf{r}_1)\epsilon_i(\mathbf{r}_2)\rangle - \langle\epsilon_i(\mathbf{r}_1)\rangle\langle\epsilon_i(\mathbf{r}_2)\rangle = \mathcal{A}^2\langle|\psi_i(\mathbf{r}_1)|^2_{\mathrm{osc}}|\psi_i(\mathbf{r}_2)|^2_{\mathrm{osc}}\rangle$ in this way [see Eq. (20)]. To be more precise, let the $\{A_\mu\}$ be uncorrelated unless the corresponding trajectories are time-reversal symmetric, or related one to each other by a bounce off the boundary of the billiard near the initial or final point of the trajectory, i.e., $[(p_x^i)_{\mu'},(p_y^i)_{\mu'}] = [\pm(p_x^i)_\mu,(p_y^i)_\mu]$ and $[(p_x^f)_{\mu'},(p_y^f)_{\mu'}]$

$=[\pm(p_x^f)_\mu,(p_y^f)_\mu]$. If the reference point $\mathbf{r}$ is taken on the boundary, and measuring the distance x from the boundary, this amounts to taking A_μ equal for these trajectories, giving

$$\mathcal{A}^2\langle[|\psi_i(\mathbf{r}_1)|^2]_{\rm osc}[|\psi_i(\mathbf{r}_2)|^2]_{\rm osc}\rangle = \frac{2\nu_W^2}{\pi^2}\sum_\mu |A_\mu|^2\cos[(k_y^f-k_y^i)(y_1-y_2)]\mathbf{cs}(p_x^f x_1/\hbar) \times \mathbf{cs}(p_x^i x_1/\hbar)\mathbf{cs}(p_x^f x_2/\hbar)\mathbf{cs}(p_x^i x_2/\hbar), \quad (60)$$

which using the sum rule [Eq. (59)] and inserting the resulting wave-function correlations in Eq. (18) gives exactly Eq. (22) derived with the random plane-wave model.

To summarize, neglecting dynamical correlations in the semiclassical approach generates a random pair of plane-waves model that, in essence is derived with usual approximations. For the problem we consider here, this model gives exactly the same result as the random plane-wave model. The random pair of plane wave is however not *ad hoc*, whereas the random plane-waves model is. This makes it possible to discuss precisely what approximations have been made, and therefore in what way we could expect the random model to differ from the purely semiclassical treatment. In particular we see that the interferences between reflected wave at the boundary is treated in the same way in both the semiclassical and the random approaches, giving rise to the same $\lambda(\theta)$ dependence. On the other hand the prefactor is related, in the semiclassical approach, to the way classical orbit with nearly matching initial and final momenta are structured around periodic orbit. This aspect is completely ignored in the random models, and we therefore cannot expect them to give exactly the correct prefactor.

V. NONCHAOTIC SYSTEMS

Included in the class of nonchaotic dynamical systems are three main subclasses: (i) the limiting case of integrable systems, all of whose dynamics are regular; (ii) near-integrable systems, characterized by having classical perturbation theory generally work well in describing its dynamics; and (iii) mixed systems, which contain an intricate mixture of both regular and chaotic dynamical regions in their phase spaces. Generally speaking, semiclassical theories and what is known vary according to each subclass. For example, trace formulae exist for integrable [46,47] and near-integrable systems [48,49] but not for mixed systems. In fact, a proper treatment of semiclassical theory for mixed systems is lacking. However, for the purpose here of investigating the properties of the set of $\{\mathcal{S}_i\}$, only the simplest level of semiclassical theory is considered. In other words, in regular dynamical regions (whether from integrable, near-integrable, or mixed systems), structures called tori are assumed to exist, which are invariant manifolds under classical motion, and possible complications from resonances, diffraction, or tunneling are ignored. In chaotic regions, only the complication of a family of marginally stable orbits is considered beyond that which was already treated in the previous section.

Unlike chaotic dynamical regions in phase space, for regular regions there are two possible overarching semiclassical approaches. In the first, particular tori quantize allowing the detailed evaluation of $\mathcal{S}_i$ for each eigenstate. This is based on the Einstein-Brillouin-Keller (EBK) scheme [50–52]. In the second, a periodic orbit trace formula results from applying a Green-function approach, much like the chaotic case. However, this Green-function approach is not given here since the information about each individual $\mathcal{S}_i$, the mean, and variance are already understandable through the EBK approach.

A. Einstein-Brillouin-Keller quantization

1. General expression for $\mathcal{S}_i$

Continuing with two dimensional billiards, each torus is characterized by two action variables (J_1,J_2), and it is always possible to choose the corresponding angles (φ_1,φ_2) such that the intersections of the torus with the boundary of the billiard are parameterized as $\varphi_1=f_\kappa(\varphi_2)$ and $\kappa=1,\ldots,\kappa_{\max}$, with $\kappa_{\max}$ as the number of bounces on the boundary for the considered torus.

An eigenstate Ψ_i is constructed on a quantizing torus $[J_1=2\pi\hbar(n_1^{(i)}+\sigma_1/4),J_2=2\pi\hbar(n_2^{(i)}+\sigma_2/4)]$, where (σ_1,σ_2) are the Maslov indices and can be expressed as

$$\Psi_i(\mathbf{r}) = \frac{1}{2\pi}\sum_\ell \sqrt{\left|\frac{\partial(\varphi_1,\varphi_2)}{\partial(x,y)}\right|_\ell}\exp\left(\frac{i}{\hbar}S_\ell(x,y)\right). \quad (61)$$

The sum runs over the various sheets of the torus projecting onto the point $\mathbf{r}=(x,y)$ and $S_\ell(x,y)$ is the corresponding action (including the Maslov phases).

Consider in greater detail, the neighborhood of the $\varphi_1=f_\kappa(\varphi_2)$ boundary. To further simplify the discussion, assume that the torus has only two sheets [corresponding to negative and positive $\varphi_1-f_\kappa(\varphi_2)$] projecting on any given point (x,y) near this boundary. The results derived under this hypothesis apply in the general case, as is justified below. Adding the two $\varphi_1<f_\kappa(\varphi_2)$ and $\varphi_1>f_\kappa(\varphi_2)$ contributions and expanding the action from the boundary as $S(x,y)=S(x=0,y)+p_x x$ generates

$$\Psi(x,y) = \frac{1}{2\pi}\sqrt{\left|\frac{\partial(\varphi_1,\varphi_2)}{\partial(x,y)}\right|}\exp\left(\frac{i}{\hbar}S(x=0,y)\right)2\mathbf{cs}(p_x x/\hbar); \quad (62)$$

assuming that the local variation of the Jacobian determinant in the direction perpendicular to the boundary can be neglected. Inserting this expression into Eq. (16) we obtain

$$\mathcal{S}_i = i\left(1\mp\frac{\mathcal{L}}{k_F\mathcal{A}}\right)\pm\tilde{\mathcal{S}}_i, \quad (63)$$

with

$$\tilde{\mathcal{S}}_i = \frac{i}{\pi^2}\int dxdy\left|\frac{\partial(\varphi_1,\varphi_2)}{\partial(x,y)}\right|\frac{J_1(2k_F x)}{k_F x}\mathbf{cs}^2(p_x x/\hbar). \quad (64)$$

If the torus has more than two sheets projecting onto the neighborhood of the boundary [in which case Eq. (62) involves a sum], the rapidly oscillating phases, $\{\exp[iS(x=0,y)/\hbar]\}$, eliminate cross terms upon integration

over y, and thus the calculation of $\tilde{\mathcal{S}}_i$ would involve just a single sum.

Changing the integration variables to (φ_2^0, τ), with τ measuring the time from the bounce on the boundary of the billiard and φ_2^0 as the angle φ_2 at that bounce, we can further simplify Eq. (64). Indeed

$$\varphi_2 = \varphi_2^0 + \omega_2 \tau, \tag{65}$$

$$\varphi_1 = f_\kappa(\varphi_2^0) + \omega_1 \tau, \tag{66}$$

with $\omega_i = \partial H / \partial \varphi_i (i=1,2)$ as the angular frequencies, and therefore the Jacobian can be expressed as $J = \left|\frac{\partial(\varphi_1,\varphi_2)}{\partial(\tau,\varphi_2^0)}\right| = |\omega_1 - \omega_2 (df_\kappa/d\varphi_2^0)|$. Noting furthermore that $x(\varphi_2,\tau) = v_F \cos[\theta(\varphi_2^0)]\tau$, the integral on the variable τ can be performed explicitly, giving

$$\tilde{\mathcal{S}}_i = \frac{i}{\pi k_F v_F} \sum_{\kappa=1}^{\kappa_{\max}} \frac{1}{2\pi} \int_0^{2\pi} d\varphi_2^0 |\omega_1 - \omega_2 (df_\kappa/d\varphi_2^0)| \lambda[\theta_\kappa(\varphi_2^0)]. \tag{67}$$

2. Circular billiard

Beyond the orders of magnitude, the explicit evaluation of the variance of the set $\{\mathcal{S}_i\}$ for integrable systems is very much system dependent as it is usually not possible to make general assumptions about the correlations between the various quantities involved $(\lambda[J_1, J_2, \theta_\kappa(\varphi_2^0)], \omega_{1,2}(J_1,J_2), df_\kappa/d\varphi_2^0[J_1,J_2,\theta_\kappa(\varphi_2^0)])$. We therefore consider now a specific system, namely, the circular billiard.

The computation of expression (67) for this billiard is made somewhat simpler because the angle θ at which trajectories bounce off the boundary is a constant for a given torus, and thus a function of the actions (J_1,J_2) only. Furthermore, for a given invariant torus, we can construct the paths on which the action variables (J_1,J_2) are constructed as the cut of the torus in the radial direction (for J_1), and the caustic (or any topologically equivalent path) for J_2. In this way, the angle φ_2 can be identified with the angle of the polar coordinates, and the boundary of the billiard can be taken as $\varphi_1 = 0$ (i.e., $f_{\kappa=\kappa_{\max}=1} \equiv 0$). Furthermore the angular frequency $\omega_1(J_1,J_2)$ can be identified with $2\pi/t(J_1,J_2)$, with $t(J_1,J_2)$ as the time between two successive bounces for trajectories of the corresponding torus. Expression (67) thus takes the simple form

$$\tilde{\mathcal{S}}_i = \frac{2i}{k_F v_F} \frac{\lambda[\theta(J_1,J_2)]}{t(J_1,J_2)}. \tag{68}$$

Quantizing tori sample uniformly the plane (J_1,J_2), and therefore statistical quantities such as average and variance should be computed with the measure $dJ_1 dJ_2$. However, using that the change of variable $(J_1,J_2,\varphi_1,\varphi_2) \to (E,\xi,\tau,p_\xi)$ introduced in Appendix B ($p_\xi \equiv p_F \sin\theta$) is canonical, implying $dJ_1 dJ_2 d\varphi_1 d\varphi_2 = dE dp_\xi d\tau d\xi$, and that for the circular billiard θ and E depend only on the action (J_1,J_2), and τ and ξ on the angles (φ_1,φ_2), one can write, in the neighborhood of the Fermi energy E_F,

$$dJ_1 dJ_2 \delta(E - E_F) \propto t(J_1,J_2) d(\sin\theta), \tag{69}$$

and thus use the probability measure

$$dP = \frac{t(\theta)}{\langle t(\theta)\rangle} d\sin(\theta), \tag{70}$$

with $\langle T(\theta)\rangle$ given by Eq. (B6) arising from the normalization (given for allowed values of $\sin\theta$ in the range $0 \le \sin\theta \le 1$).

One can in this way recover in the particular case of the circular billiard the general expression [Eq. (17)] of the mean value $\langle \mathcal{S}_i \rangle$. Indeed

$$\langle \tilde{\mathcal{S}}_i \rangle = \frac{2i}{k_F} \frac{\mathcal{L}}{\pi \mathcal{A}} \langle \lambda(\theta) \rangle_\theta \text{ and } \langle \mathcal{S}_i \rangle = i\left(1 \mp \frac{\mathcal{L}}{k_F \mathcal{A}}\right) \pm 2i \frac{\mathcal{L}}{\pi k_F \mathcal{A}} \left(\frac{\pi}{2} \pm 1\right) = i\left(1 + \frac{2\mathcal{L}}{\pi k_F \mathcal{A}}\right). \tag{71}$$

Similarly, the expression for the variance reduces to

$$\begin{aligned} \mathrm{Var}[\mathcal{S}_i] &= \frac{4i^2 \mathcal{L}}{k_F^2 v_F \pi \mathcal{A}} \int_0^1 d(\sin\theta) \frac{\lambda^2(\theta)}{T_1(\theta)} - \left[\frac{i\mathcal{L}}{k_F \mathcal{A}}\left(1 \pm \frac{2}{\pi}\right)\right]^2 \\ &= \frac{4i^2}{k_F^2 \pi R^2} \int_0^1 \frac{d(\sin\theta)}{\cos\theta} \frac{(1 \pm \sin\theta)^2}{\cos^2\theta} - \left[\frac{2i}{k_F R}\left(1 \pm \frac{2}{\pi}\right)\right]^2. \end{aligned} \tag{72}$$

As before, the constant for Dirichlet boundary conditions is quite small, and the divergence of Neumann boundary conditions increases the order. In this case, the effect is greater than logarithmic. Using the same cutoff for the Neumann case as at the end of Sec. III B and that $i \approx \mathcal{A} k_F^2 / 4\pi$, we obtain

$$\mathrm{Var}[\mathcal{S}_i] = i \times \begin{cases} \frac{2}{\pi} - \frac{1}{2} - \left(1 - \frac{2}{\pi}\right)^2 \approx 0.00457 & \text{Dirichlet} \\ -\frac{2}{\pi} - \frac{1}{2} + \pi^{1/2} i^{1/4} - \left(1 - \frac{2}{\pi}\right)^2 & \text{Neumann}. \end{cases} \tag{73}$$

Thus the variance scales proportionally to i for Dirichlet boundary conditions and $i^{5/4}$ for Neumann boundary conditions.

B. Bouncing ball modes in the stadium billiard

Even for fully chaotic systems, it is possible to have a situation where some (with vanishing measure) of the trajectories behave more like those of integrable systems. An example is provided by the bouncing ball orbits of the stadium billiard [53]. Tanner [54] showed that for the purposes of a semiclassical theory of eigenstates, the phase space in the neighborhood of the bouncing ball orbits behaved much like an island of regular motion and that families of orbits that cannot be taken as isolated contribute in essential ways. This greatly complicates the desire for a rigorous semiclassical

theoretical approach. Although these states can be thought of as EBK-like states like those studied in Sec. V A, they do get connected through diffractive terms to the chaotic states, and thus some of them behave more like resonances rather than individual quantized states.

A complete semiclassical description is beyond the scope of this study. Indeed, as mentioned in the beginning of Sec. V, as many dynamical system complications as possible are being neglected here. Instead of attempting a rigorous semiclassical theory for the bouncing ball modes, a rough approximation is given instead. To be specific, we consider here the even-even symmetry states of a stadium billiard with Dirichlet boundary conditions or equivalently a symmetry-reduced quarter stadium with Dirichlet boundary conditions on the original boundaries and Neumann boundary conditions on the symmetry lines. To start, consider the eigenstates of a rectangle with one side length equivalent to the side length L_s of the symmetry-reduced quarter stadium and the other, the radius of curvature R. These states can be used to give an approximation to the bouncing ball modes. In essence, the bouncing ball modes with few nodes along the side length (ignoring mixing into the chaotic states) vanish quickly upon entering the quarter circular end cap. A quantization along the side length direction with Dirichlet boundary conditions on the side entering the end cap and along the side length itself is a good starting point. Since our calculations have been done for even-even symmetry eigenstates, consider Neumann boundary conditions for the remaining two sides. The normalized states are given in the Cartesian coordinates by

$$|\Psi_i(q_1,q_2)|^2 = \frac{4}{RL_s}\cos^2\left(\frac{2m+1}{2L_s}\pi q_1\right)\cos^2\left(\frac{2n+1}{2R}\pi q_2\right), \tag{74}$$

where the origin is the corner. m is a small integer, say 0,1,2,3, or so, and most of the kinetic energy is in the other direction and so n is a large integer.

To write the equation for the $\mathcal{S}_i$, the coordinate system of the state must be rotated and translated to the boundary coordinate system used for the Friedel oscillations separately along the two symmetry lines and the side length. This gives three terms to evaluate for the bouncing ball contributions,

$$\begin{aligned}\mathcal{S}_i^{(\mathrm{bb})} &= i\left(1+\frac{\mathcal{L}_D-\mathcal{L}_N}{k_F\mathcal{A}}\right)\\ &+\frac{2i}{L_s}\int_0^\infty dx\frac{J_1(2k_Fx)}{k_Fx}\cos^2\left(\frac{2m+1}{2L_s}\pi x\right)\\ &+\frac{2i}{R}\int_0^\infty dx\frac{J_1(2k_Fx)}{k_Fx}\left[\cos^2\left(\frac{2n+1}{2R}\pi x\right)\right.\\ &\left.+\sin^2\left(\frac{2n+1}{2R}\pi x\right)\right] = i\left(1+\frac{\mathcal{L}_D-\mathcal{L}_N}{k_F\mathcal{A}}\right)+\frac{2i}{k_FR}\\ &+\frac{i}{k_FL_s}\left(1+\sqrt{1-\left[\frac{(2m+1)\pi}{4k_FL_s}\right]^2}\right)\mathcal{S}_i^{(\mathrm{bb})}-\langle\mathcal{S}_i\rangle\end{aligned}$$

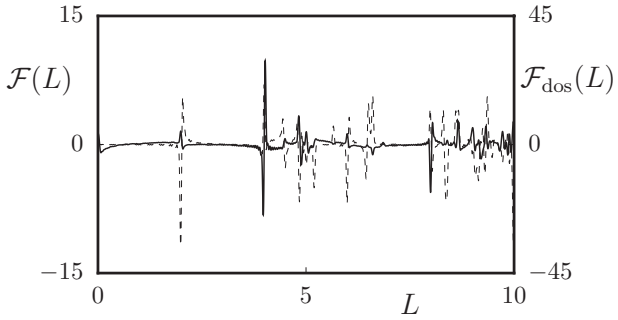

FIG. 7. Fourier transform of $\mathcal{S}_i-\langle\mathcal{S}_i\rangle$ and the density of states from the even-even stadium eigenstates using Dirichlet boundary conditions. The dashed line is for the density of states (which has a different vertical scale shown at the right side).

$$= \frac{i}{k_F\mathcal{A}}\left[\mathcal{L}_D-\mathcal{L}_N-\frac{2\mathcal{L}}{\pi}+2\mathcal{A}\left(\frac{1}{R}+\frac{1}{L_s}\right)\right], \tag{75}$$

where the straightforward integrals over the y coordinates have been evaluated before writing the first expression, and $\mathcal{L}_D=L_s+\pi R/2$ and $\mathcal{L}_N=L_s+2R$ are the perimeter lengths with Dirichlet and Neumann boundary conditions, respectively. In the last expression, the overall mean Eq. (17) is subtracted and the square root reduces to unity since bouncing balls with significant momentum toward and away from the end cap do not exist.

There are a number of interesting consequences of Eq. (75). The last line captures the scale of the deviation from the mean. Putting in the parameters used for the stadium calculations of Figs. 2 and 3 ($R=L_s=1$) generates a growing expected deviation from the mean that hits about 30 for $i=2000$. This result also implies that $\mathcal{S}_i$ for the nonbouncing ball modes fluctuate about a negative bias given by

$$\begin{aligned}\mathcal{S}_i^{(\text{non bb})}-\langle\mathcal{S}_i\rangle &= \frac{-f_{\mathrm{bb}}}{1-f_{\mathrm{bb}}}\frac{i}{k_F\mathcal{A}}\\ &\times\left[\mathcal{L}_D-\mathcal{L}_N-\frac{2\mathcal{L}}{\pi}+2\mathcal{A}\left(\frac{1}{R}+\frac{1}{L_s}\right)\right],\end{aligned} \tag{76}$$

where the fraction of bouncing ball modes is denoted f_{bb}. The best known estimate of f_{bb} for the stadium billiard to our knowledge comes from Tanner [54], which implies that $f_{\mathrm{bb}}\approx\gamma[\frac{2}{\pi(\gamma+\pi/4)}]^{3/4}i^{-1/4}$; we have introduced the ratio $\gamma=L_s/R$ and used that $4\pi i=\mathcal{A}k_F^2$. For other systems with bouncing ball modes, their fraction may scale differently [55]. The results of Eqs. (75) and (76) are given by the dashed and solid lines in Fig. 2(b). The dashed (upper) line crosses right through the neighborhood of the peak values. For such a rough approximation, Eq. (75) is quite good. In addition, the solid (lower) line captures the negative bias implied for the nonbouncing ball modes quite well.

Second, to the level of approximation here, any of the bouncing ball modes contribute fairly equally locally in energy (determined by the quantum number n); i.e., there is almost no dependence on sequence number m. Although, the peak values from the bouncing balls do not appear to be

constant in the figure, presumably due to weak admixtures of chaotic states, this feature greatly simplifies a calculation of the fluctuations. The variance can be inferred by noting the following: (i) the square of the bouncing ball deviation from the mean multiplied by their fraction denoted $f_{\rm bb}$ gives their contribution and (ii) the contribution of the remaining $1-f_{\rm bb}$ nonbouncing ball modes can be taken as the square of the average amount they must each be in deficit of the mean plus the [subleading] variance from the chaotic system results. The combined consequences lead to the expression

$$\mathrm{Var}[\mathcal{S}_i] = \frac{f_{\rm bb}}{1-f_{\rm bb}}\frac{i}{4\pi\mathcal{A}}\left[\mathcal{L}_D - \mathcal{L}_N - \frac{2\mathcal{L}}{\pi} + 2\mathcal{A}\left(\frac{1}{R}+\frac{1}{L_s}\right)\right]^2 + \mathrm{Var}[\mathcal{S}_i]_{\rm chaotic},$$

with

$$\mathrm{Var}[\mathcal{S}_i]_{\rm chaotic} = \frac{k_F\mathcal{L}}{2\pi^3}\left[(2\ln 2 - 1) - \left(\frac{\pi}{2}-1\right)^2\right] + \frac{2k_F\mathcal{L}_N}{\pi^3}\left(\ln\frac{\pi k_F\mathcal{A}}{2\mathcal{L}} - \frac{\pi}{2}\right). \quad (77)$$

Taking account of the decreasing fraction of bouncing ball modes with increasing i, the variance scales as $i^{3/4}$. See Fig. 3 for a comparison of this formula with $\mathrm{Var}[\mathcal{S}_i]$ for the even-even eigenstates of the stadium billiard. Again, the rudimentary approach here captures the main behavior fairly well.

To conclude this subsection on the bouncing ball orbits, a few remarks are in order. First, we stress that although the classical dynamics of the stadium billiard is, mathematically speaking, purely chaotic as far as $\mathcal{S}_i$ statistics are concerned the existence of the marginally stable bouncing ball family makes this system behave very much like an integrable billiard. In particular the scale of the fluctuations are order of magnitude larger than for the "genuine" chaotic billiard considered in Secs. III and IV. Second, because of the presence of two classes of states with drastically different properties, the covariance among the $\mathcal{S}_i$ is, again in contrast with genuine chaotic systems, nonzero. Furthermore, both the variance and the covariance show an energy dependent structure which complicates significantly the extraction of these quantities from the locally smoothed $\overline{\mathcal{S}_i}_{\Delta N}$ as was done in Sec. IV.

As a final remark, although the periodic orbit formula is not derived here, Fig. 7 is shown for completeness. As in Fig. 6, the results are compared between the density of states and the $\{\mathcal{S}_i\}$. Again, the peaks are in the same positions, i.e., those determined by periodic orbits but with differing amplitudes. The importance of the bouncing ball modes is quite visible.

VI. DISCUSSION

The mean and variance of the quantities $\{\mathcal{S}_i\}$ treated in [26] and in greater detail in this paper have been introduced as examples of a nonlocal class of statistical measures with physical relevance; the $\{\mathcal{S}_i\}$ are connected to the addition spectrum of quantum dots. By no means should they be taken as the only possible measures representing this class. Indeed, in recent works on finite-size fluctuation properties in ultracold Fermi gases [12,56], involving fluctuations in the Bardeen-Cooper-Schrieffer pairing gap, a quantity was introduced for the order parameter that is similar to the $\{\mathcal{S}_i\}$, although with additional complications. Not surprisingly, several common features are found for both quantities. As the fluctuations are dominated by a term arising from the interplay of the Friedel and eigenstate oscillations, there is a significant decrease in fluctuation magnitude due to Dirichlet boundary conditions, either through reduction or even vanishing of the prefactor of the leading term in k_FL. In the case of the $\{\mathcal{S}_i\}$, the prefactor is decreased by more than an order of magnitude with respect to the prefactor for Neumann boundary conditions. Another critical feature is the role of dynamics in the scale of the fluctuations. Chaotic dynamical systems lead to a fluctuation scale of lower order in k_FL than integrable or mixed dynamical systems. Again, this leads to a fluctuation scale decreased by an order of magnitude or more. The decrease in scale for chaotic systems can be traced to an ergodic nature of the individual eigenstates. Conversely, the much larger fluctuation scale for integrable and mixed phase space systems, suggests the possibility of new physics associated with more regular dynamics or the possibility of measurements that can be used to deduce information about the dynamics.

The $i^{1/2}\propto k_F\mathcal{A}/\mathcal{L}$ (or $i^{1/2}\ln i$) dependence for chaotic systems, and faster-growing dependence for integrable systems, implies that the fluctuations embodied in $\mathrm{Var}[\mathcal{S}_i]$ in fact grow with the size of the system, becoming eventually larger than of order unity. This implies that the corresponding residual interaction contributions will in that case become larger than the mean level spacing Δ. In other words, since Δ is the energy scale set by the one particle energies, the fluctuations in the residual interactions may become large enough that they generate a modification in the ground-state orbital occupation number and more generally reach a point where a first-order perturbation treatment of the interactions is not adequate.

Returning to the two theoretical approaches included here—a random plane-wave model for chaotic systems and semiclassical theory, whatever the dynamics—we have seen that the basic random plane-wave model is intrinsically less powerful than semiclassical theory, but on the other hand, it is technically much simpler to implement. Surprisingly, given the excellent results it generates in other contexts, the random plane-wave model here displays a couple of significant faults. The most simple to track down is the effect of having its normalization be across the ensemble as opposed to the individual eigenstates. For chaotic systems, this led directly to the replacement of the mean square of $\lambda(\theta)$ by its variance. Inclusion of the variance improved the theory considerably as the mean square largely overestimated the prefactor. In addition, the proper treatment of dynamical correlations in the semiclassical theory led to a factor 2 increase in the prefactor constant. Truth be told, for the cardioid billiard example, the results seem to agree better without the factor 2 (see Fig. 6), but a concerted search for an error in the semiclassical calculation never resulted in its removal.

Finally, it is important to be aware of some consequences of decompositions such as given in Eq. (9). The separation of

average and fluctuating parts of a nonlocal statistical measure may not be the full story from a physical perspective. In fact, this is the case for the $\{\mathcal{S}_i\}$ treated here. As noted earlier, the mean of $\mathcal{S}_i$ does not lead to any modification of the ground-state occupations numbers as its effects gets cancelled. On the other hand, the fluctuating part of $\mathcal{S}_i$ does affect the ground state, but there are two components. The leading order fluctuations that come from the use of the term $N_{\text{sec}}(\mathbf{r};E_i^+)$ in the fluctuation expressions is essentially a mean-field effect, analogous to scrambling. These fluctuations, if large enough, can reorder the filling of the single-particle levels. They do not however lead to high spin states or other unusual behaviors. The remaining term $\delta N(\mathbf{r};E_i^+)$ is responsible for exotic physics in those cases where it is sufficiently large. As the focus throughout this paper was on developing the theory of the nonlocal statistical measures themselves, the leading behaviors have been emphasized, which though dominant are not necessarily the only ones that deserve to be considered—that depends on the physical context (other types of problems exist, such as the fluctuations of superconducting gap mentioned earlier, where the dominant terms in the relevant nonlocal statistical measures do contain all the important physics). Therefore, revisiting the fluctuation-fluctuation term involving $\delta N(\mathbf{r};E_i^+)$ will sometimes be important but is left for future work.

ACKNOWLEDGMENTS

We gratefully acknowledge discussions with Barbara Dietz-Pilatus and Thomas Friedrich. One of us (S.T.) gratefully acknowledges support from the U.S. National Science Foundation under Grant No. PHY-0555301, and one of us (A.B.) gratefully acknowledges support from the DFG under Contract No. FOR760.

APPENDIX A: SECOND-ORDER TERMS IN THE AVERAGE PROPERTIES OF THE $\mathcal{S}_i$

There are second-order terms in the computation of the average properties of the S_i coming from the boundary, which are given here. Although, the other second-order terms from the curvature and boundary discontinuities are not being derived and hence this calculation is incomplete, the numerical calculations necessary to isolate the average behavior before calculating the variance or covariance are improved by including them. Therefore, an account is given here.

The decomposition of Eq. (9) giving $\delta N(\mathbf{r};E_i^+)$ implies

$$\delta N(\mathbf{r};E_i^+) = \sum_{j\le i} |\psi_j(\mathbf{r})|^2 - \langle |\psi_j(\mathbf{r})|^2\rangle. \tag{A1}$$

Substituting the relations from Eqs. (9) and (15) and integrating the constant terms gives

$$\mathcal{S}_i = i \pm \frac{1}{\mathcal{A}}\int d\mathbf{r} \times\left[\frac{i}{\left(1\pm\frac{\mathcal{L}}{k\mathcal{A}}\right)}\frac{J_1(2k_Fx)}{k_Fx}\epsilon_i(\mathbf{r}) \pm \mathcal{A}\delta N(\mathbf{r};E)\epsilon_i(\mathbf{r})\right]. \tag{A2}$$

The last term merits some discussion: its leading behavior is seen to be 2 orders weaker than the overall expression and is straightforward to evaluate because only its leading contribution is required. Under the operation of taking the expectation value, the only surviving term is

$$\langle \delta N(\mathbf{r};E)\epsilon_i(\mathbf{r})\rangle = \mathcal{A}\langle[|\psi_i(\mathbf{r})|^2 - \langle|\psi_i(\mathbf{r})|^2\rangle]^2\rangle, \tag{A3}$$

so that after integration over space, this is essentially equivalent to $\langle M_{ii}\rangle - \langle M_{ij}\rangle$. Indeed, the local Gaussian random behavior is uncorrelated from state to state in the random plane-wave model so that the only surviving term comes from the ith state with itself, all others vanishing. Locally, before squaring and taking the expectation value, the expression on the rhs of Eq. (A3) can be thought of as being like the square of a zero-mean unit-variance Gaussian random variable with unity subtracted. However, it does have a variance, which is position-dependent and given by the right-hand side of Eq. (14); i.e., the rhs acts as an envelope. Inside of the billiard (excluding the semiclassically vanishing boundary region), its value is however constant and equal to the inverse of $\mathcal{A}$ to leading order. This generates a constant, equal to 2, after integration. Therefore, the expectation value of $\mathcal{S}_i$ is approximately

$$\begin{aligned}\langle \mathcal{S}_i\rangle &= i + 2 \pm \frac{i}{\mathcal{A}\left(1\pm\frac{\mathcal{L}}{k_F\mathcal{A}}\right)}\int d\mathbf{r}\frac{J_1(2k_Fx)}{k_Fx}\langle\epsilon_i(\mathbf{r})\rangle \\ &= i + 2 + \frac{i}{\mathcal{A}\left(1\pm\frac{\mathcal{L}}{k_F\mathcal{A}}\right)\left(1\pm\frac{\mathcal{L}}{2k_F\mathcal{A}}\right)}\int d\mathbf{r}\frac{J_1(2k_Fx)}{k_Fx} \times\left[J_0(2k_Fx) - \frac{\mathcal{L}}{2k_F\mathcal{A}}\right] \\ &= i\left(1 + \frac{\mathcal{L}}{k_F\mathcal{A}}\frac{1}{\left(1\pm\frac{\mathcal{L}}{k_F\mathcal{A}}\right)\left(1\pm\frac{\mathcal{L}}{2k_F\mathcal{A}}\right)}\left[\frac{2}{\pi} - \frac{\mathcal{L}}{2k_F\mathcal{A}}\right]\right) \\ &\quad + 2 = i\left[1 + \frac{2\mathcal{L}}{\pi k_F\mathcal{A}} \mp \left(\frac{3}{\pi}\pm\frac{1}{2}\right)\frac{\mathcal{L}^2}{k_F^2\mathcal{A}^2}\right] + 2,\end{aligned} \tag{A4}$$

where we choose $k_F = \sqrt{2mE_i}/\hbar$. Interestingly enough, if a length $\mathcal{L}_D$ of the boundary follows Dirichlet conditions and a length $\mathcal{L}_N$ follows Neumann conditions, it is not correct just to make the substitution $\pm\mathcal{L}\to\mathcal{L}_N-\mathcal{L}_D$. Rather, the above expression becomes

$$\langle \mathcal{S}_i\rangle = i\left[1 + \frac{2\mathcal{L}}{\pi k_F\mathcal{A}} - \left(\frac{3\mathcal{L}}{\pi} + \frac{\mathcal{L}_N-\mathcal{L}_D}{2}\right)\frac{\mathcal{L}_N-\mathcal{L}_D}{k_F^2\mathcal{A}^2}\right] + 2 \tag{A5}$$

after redoing the algebra. The distinction arises because some of the correction terms depend on the sign of the boundary conditions, whereas other correction terms depend on the sign squared.

APPENDIX B: MEAN LENGTH OF A TRAJECTORY BETWEEN TWO SUCCESSIVE BOUNCES

This appendix briefly rederives Eq. (46), which gives the mean length of a trajectory between two successive bounces off the boundary of a billiard. While this is a well-known result (see [57] and references therein), several equations used in the derivation are needed in the main text. The result can actually be obtained by computing in two different ways the energy surface volume of the billiard

$$V(E) = \int d\mathbf{p}d\mathbf{r}\,\delta[E - H(\mathbf{r},\mathbf{p})], \tag{B1}$$

with $H(\mathbf{p},\mathbf{r})=\mathbf{p}^2/2m+V(\mathbf{r})$ and $V(\mathbf{r})=0$ inside the billiard and ∞ outside. The first way is to perform this integral with the original coordinates $(\mathbf{r},\mathbf{p})$, giving $V(E)=2\pi m\mathcal{A}$.

The second way to perform this integral is to use another set of coordinates, constructed as follows. Any point $(\mathbf{r},\mathbf{p})$ of the billiard's phase space can be considered as belonging to a trajectory which has last bounced off the boundary a time τ ago at a location on the boundary labeled by the curvilinear abscissa ξ. Denote $\mathbf{r}_0(\xi)$ the corresponding point on the boundary and introduce the action

$$S(r_1,r_2,\tau,\xi) \overset{\text{def}}{=} \int_{\mathbf{r}_0(\xi)}^{\mathbf{r}=(r_1,r_2)} L(\tau')d\tau', \tag{B2}$$

with $L=\mathbf{p}\dot{\mathbf{r}}-H$ as the Lagrangian function. Since $\partial S/\partial\mathbf{r}=\mathbf{p}$, $S(r_1,r_2,\tau,\xi)$ can be used as the generating function of the canonical transformation

$$(\mathbf{r},\mathbf{p}) \to (\mathbf{Q},\mathbf{P}), \tag{B3}$$

with $\mathbf{Q}=(\xi,\tau)$. The new momentum coordinates are thus given by

$$P_1 = -\frac{\partial S}{\partial Q_1} = -\frac{\partial S}{\partial \tau} = -E,$$

$$P_2 = -\frac{\partial S}{\partial Q_2} = -\frac{\partial S}{\partial \xi} = p_\xi,$$

with p_ξ as the projection of the momentum $\mathbf{p}$ on the direction parallel to the boundary at ξ.

As Eq. (B3) is a canonical transformation, $d\mathbf{r}d\mathbf{p}=d\mathbf{Q}d\mathbf{P}$ and the energy surface volume is

$$V(E) = \int d\xi dp_\xi dE d\tau \delta(E - H). \tag{B4}$$

Performing the straightforward integration over energy and noting that for given (ξ,p_ξ) the integral over $d\tau$ yields the time of travel $t(\xi,p_\xi)$ of the corresponding trajectory between ξ and the following bounce gives

$$V(E) = \int d\xi dp_\xi t(\xi,p_\xi) = 2p\mathcal{L}\bar{t}, \tag{B5}$$

with $p=\sqrt{2mE}$ and $\bar{t}$ as the mean time of travel between two successive bounces. Identifying this expression with the one obtained using the original coordinate system gives

$$\frac{p}{m}\bar{t} = \frac{\pi\mathcal{A}}{\mathcal{L}}, \tag{B6}$$

and finally, using $p/m=|\dot{\mathbf{r}}|$, one finds Eq. (46).

APPENDIX C: NORMALIZATION CORRECTIONS TO EQ. (39)

Note that in Eq. (39) only the terms which are of leading order *near the boundary* have been kept. Others have been neglected which, though smaller near the boundary, are of the same size as some of the terms kept when integrated over the full area of the billiard. In particular, as it is, Eq. (39) gives the normalization of the wave function only up to $\mathcal{L}/k_F\mathcal{A}$ corrections. If however $\rho_W(E)(1\pm\mathcal{L}/k_F\mathcal{A})$ is used rather than $\rho_W(E)$ for the smooth part of the density of states, Eq. (35) is replaced by

$$\begin{aligned}\mathcal{A}\overline{|\Psi_i(\mathbf{r})|^2}_{\Delta N} - 1 = {} & \pm J_0(2k_Fx) \mp \frac{\mathcal{L}}{2k_F\mathcal{A}} + \frac{\mathcal{L}^2}{4k_F^2\mathcal{A}^2} \\ & - \frac{\mathcal{L}}{2k_F\mathcal{A}} J_0(2k_Fx) \frac{1}{\mathcal{A}^2\nu_W^2} \overline{\rho_{\text{osc}}^2(E)}_{\Delta E} \\ & + \frac{1}{\pi\mathcal{A}\nu_W^2} \overline{\rho_{\text{osc}}(E)}_{\Delta E}\, \text{Im}\, \overline{\tilde{G}_{\text{osc}}(\mathbf{r},\mathbf{r},E)}_{\Delta E} \\ & - \frac{1 \mp \dfrac{\mathcal{L}}{2k_F\mathcal{A}}}{\pi\nu_W} \text{Im}\, \overline{\tilde{G}_{\text{osc}}(\mathbf{r},\mathbf{r},E)}_{\Delta E} \\ & - \frac{1 \pm J_0(2k_Fx) \mp \dfrac{\mathcal{L}}{k_F\mathcal{A}}}{\mathcal{A}\nu_W} \overline{\rho_{\text{osc}}(E)}_{\Delta E}. \end{aligned} \tag{C1}$$

Integration over the rhs gives precisely zero with each pair of terms from the beginning in order, respectively, canceling each other. Thus, the eigenstate normalization is unity from the leading constant term on the left-hand side.

[1] O. Bohigas, S. Tomsovic, and D. Ullmo, Phys. Rep. **223**, 43 (1993).
[2] I. L. Aleiner and A. I. Larkin, Phys. Rev. E **55**, R1243 (1997).
[3] A. D. Mirlin, Phys. Rep. **326**, 259 (2000).
[4] H. Schomerus and P. Jacquod, J. Phys. A **38**, 10663 (2005).
[5] O. Bohigas, M. J. Giannoni, and C. Schmit, Phys. Rev. Lett. **52**, 1 (1984).
[6] O. Bohigas, in *Chaos and Quantum Physics*, edited by M. J.

Giannoni, A. Voros, and J. Jinn-Justin (North-Holland, Amsterdam, 1991), pp. 87–199.
[7] M. L. Mehta, *Random Matrices*, 3rd ed. (Elsevier, Amsterdam, 2004).
[8] M. V. Berry, J. Phys. A **10**, 2083 (1977).
[9] A. Voros, in *Stochastic Behaviour in Classical and Quantum Hamiltonian Systems*, edited by G. Casati and G. Ford (Springer-Verlag, Berlin, 1979), p. 334.
[10] D. Ullmo, T. Nagano, and S. Tomsovic, Phys. Rev. Lett. **90**, 176801 (2003).
[11] M. Miller, D. Ullmo, and H. U. Baranger, Phys. Rev. B **72**, 045305 (2005).
[12] A. M. Garcia-Garcia, J. D. Urbina, E. A. Yuzbashyan, K. Richter, and B. L. Altshuler, Phys. Rev. Lett. **100**, 187001 (2008).
[13] U. Sivan, R. Berkovits, Y. Aloni, O. Prus, A. Auerbach, and G. Ben-Yoseph, Phys. Rev. Lett. **77**, 1123 (1996).
[14] F. Simmel, T. Heinzel, and D. A. Wharam, Europhys. Lett. **38**, 123 (1997).
[15] S. R. Patel, S. M. Cronenwett, D. R. Stewart, A. G. Huibers, C. M. Marcus, C. I. Duruöz, J. S. Harris, K. Campman, and A. C. Gossard, Phys. Rev. Lett. **80**, 4522 (1998).
[16] F. Simmel, D. Abusch-Magder, D. A. Wharam, M. A. Kastner, and J. P. Kotthaus, Phys. Rev. B **59**, R10441 (1999).
[17] S. Lüscher, T. Heinzel, K. Ensslin, W. Wegscheider, and M. Bichler, Phys. Rev. Lett. **86**, 2118 (2001).
[18] S. Tarucha, D. G. Austing, T. Honda, R. J. van der Hage, and L. P. Kouwenhoven, Phys. Rev. Lett. **77**, 3613 (1996).
[19] Y. M. Blanter, A. D. Mirlin, and B. A. Muzykantskii, Phys. Rev. Lett. **78**, 2449 (1997).
[20] D. Ullmo and H. U. Baranger, Phys. Rev. B **64**, 245324 (2001).
[21] G. Usaj and H. U. Baranger, Phys. Rev. B **64**, 201319(R) (2001).
[22] G. Usaj and H. U. Baranger, Phys. Rev. B **66**, 155333 (2002).
[23] I. L. Aleiner, P. W. Brouwer, and L. I. Glazman, Phys. Rep. **358**, 309 (2002).
[24] D. Ullmo, H. Jiang, W. Yang, and H. U. Baranger, Phys. Rev. B **70**, 205309 (2004).
[25] D. Pines and P. Nozières, *Theory of Quantum Liquids* (Benjamin, New York, 1966), Vol. I.
[26] S. Tomsovic, D. Ullmo, and A. Bäcker, Phys. Rev. Lett. **100**, 164101 (2008).
[27] M. C. Gutzwiller, J. Math. Phys. **12**, 343 (1971) and references therein.
[28] M. C. Gutzwiller, *Chaos in Classical and Quantum Mechanics* (Springer-Verlag, New York, 1990).
[29] A. Bäcker, R. Schubert, and P. Stifter, Phys. Rev. E **57**, 5425 (1998); **58**, 5192(E) (1998).
[30] D. Ullmo, Rep. Prog. Phys. **71**, 026001 (2008).
[31] L. Hörnander, *The Analysis of Linear Partial Differential Operators III* (Springer, Berlin, 1985), see theorem 17.5.10.
[32] M. S. Longuet-Higgins, J. Mar. Res. **11**, 1245 (1952).
[33] E. B. Bogomolny, Physica D **31**, 169 (1988).
[34] M. V. Berry, J. Phys. A **35**, 3025 (2002).
[35] M. Robnik, J. Phys. A **16**, 3971 (1983).
[36] M. Robnik, J. Phys. A **17**, 1049 (1984).
[37] A. Bäcker, F. Steiner, and P. Stifter, Phys. Rev. E **52**, 2463 (1995).
[38] L. A. Bunimovich, Funct. Anal. Appl. **8**, 254 (1974).
[39] L. A. Bunimovich, Commun. Math. Phys. **65**, 295 (1979).
[40] S. Tomsovic and E. J. Heller, Phys. Rev. E **47**, 282 (1993).
[41] A. Bäcker and R. Schubert, J. Phys. A **35**, 539 (2002).
[42] A. M. Ozorio de Almeida, *Hamiltonian Systems: Chaos and Quantization* (Cambridge University Press, Cambridge, 1988).
[43] J. D. Urbina and K. Richter, Eur. Phys. J. Spec. Top. **145**, 255 (2007).
[44] L. Kaplan and Y. Alhassid, Phys. Rev. B **78**, 085305 (2008).
[45] N. Argaman, Phys. Rev. B **53**, 7035 (1996).
[46] M. V. Berry and M. Tabor, Proc. R. Soc. London, Ser. A **349**, 101 (1976).
[47] M. V. Berry and M. Tabor, J. Phys. A **10**, 371 (1977).
[48] S. Tomsovic, M. Grinberg, and D. Ullmo, Phys. Rev. Lett. **75**, 4346 (1995).
[49] D. Ullmo, M. Grinberg, and S. Tomsovic, Phys. Rev. E **54**, 136 (1996).
[50] A. Einstein, Verh. Dtsch. Phys. Ges. **19**, 82 (1917); english translation by C. Jaffe, JILA Report No. 116, 1980 (unpublished).
[51] L. Brillouin, C. R. Acad. Sci. **183**, 24 (1926).
[52] J. B. Keller, Ann. Phys. (N.Y.) **4**, 180 (1958).
[53] M. Sieber, U. Smilansky, S. Creagh, and R. G. Littlejohn, J. Phys. A **26**, 6217 (1993).
[54] G. Tanner, J. Phys. A **30**, 2863 (1997).
[55] A. Bäcker, R. Schubert, and P. Stifter, J. Phys. A **30**, 6783 (1997).
[56] H. Olofsson, S. Äberg, and P. Leboeuf, Phys. Rev. Lett. **100**, 037005 (2008).
[57] N. Chernov, J. Stat. Phys. **88**, 1 (1997).